

Higgs mediated flavor changing neutral currents in warped extra dimensions

Aleksandr Azatov, Manuel Toharia, and Lijun Zhu

Maryland Center for Fundamental Physics, Department of Physics, University of Maryland, College Park, Maryland 20742, USA

(Received 6 July 2009; published 20 August 2009)

In the context of a warped extra dimension with standard model fields in the bulk, we obtain the general flavor structure of the Higgs couplings to fermions. These couplings will be generically misaligned with respect to the fermion mass matrix, producing large and potentially dangerous flavor changing neutral currents. As recently pointed out [K. Agashe and R. Contino, arXiv:0906.1542.], a similar effect is expected from the point of view of a composite Higgs sector, which corresponds to a four-dimensional theory dual to the five-dimensional setup by the AdS/CFT correspondence. We also point out that the effect is independent of the geographical nature of the Higgs (bulk or brane localized), and specifically that it does not go away as the Higgs is pushed towards the IR boundary. The flavor changing neutral currents mediated by a light enough Higgs (especially their contribution to ϵ_K) could become of comparable size as the ones coming from the exchange of Kaluza-Klein gluons. Moreover, both sources of flavor violation are complementary since they have inverse dependence on the five-dimensional Yukawa couplings, such that we cannot decouple the flavor violation effects by increasing or decreasing these couplings. We also find that for Kaluza-Klein scales of a few TeV, the Higgs couplings to third generation fermions could experience suppressions of up to 40% while the rest of diagonal couplings would suffer much milder corrections. Potential LHC signatures like the Higgs flavor violating decays $h \rightarrow \mu\tau$ or $h \rightarrow tc$, or the exotic top decay channel $t \rightarrow ch$, are finally addressed.

DOI: 10.1103/PhysRevD.80.035016

PACS numbers: 14.80.Cp, 11.10.Kk

I. INTRODUCTION

Introducing a warped extra dimension in such a way as to create an exponential scale hierarchy between the two boundaries of the extra dimension [1] has generated a lot of attention in the recent years as a novel approach to solve the hierarchy problem. By placing the standard model (SM) fermions in the bulk of the extra dimension it was then realized that one can simultaneously address the flavor hierarchy puzzle of the SM [2,3]. The electroweak precision tests put important bounds on the scale of new physics but by introducing custodial symmetries [4] one can have it around few TeV [4–7].

In this paper we will study the class of models in which all the SM fields are in the bulk and the hierarchies in masses and mixings in the fermion sector are explained by small overlap integrals between fermion wave functions and the Higgs wave function along the extra dimension. This scenario can lead to the observed fermionic masses without any hierarchies in the initial five-dimensional (5D) Lagrangian, so that our fundamental 5D Yukawa couplings have no structure and are all of the same order. Another interesting feature of these models is that the contributions to low energy observables coming from the exchange of heavy Kaluza-Klein (KK) states will be suppressed by the so-called “Randall-Sundrum (RS) Glashow-Iliopoulos-Maiani” mechanism [8,9]. In spite of this, it was still found that $\Delta F = 2$ processes push the mass of the KK excitations to be above ~ 10 TeV [10–14], making it very hard to produce and observe them at the LHC [15–17]. These bounds coming from flavor violation in low energy ob-

servables can be avoided by introducing additional flavor symmetries [12,13,18,19]. Another way to relax these low energy constraints is to promote the Higgs to be a 5D bulk field (instead of being brane localized). In this situation the bounds from ϵ_K could allow masses of the lowest KK gluon to be as low as ~ 3 TeV, although combining this result with the bounds from dipole moment operators ($b \rightarrow s\gamma$, $s \rightarrow dg$) pushes back the KK scale to be above ~ 5 TeV [20,21]. A similar tension was found in the lepton sector in [22].

It has recently been pointed out that in the context of a composite Higgs sector of strong dynamics, one generically expects some amount of flavor changing neutral currents (FCNCs) mediated by the Higgs [23] (from an effective field theory point of view see also the earlier works [24–27]). In the 5D picture, the presence of KK fermion states will actually produce a misalignment between the Higgs Yukawa couplings and the SM fermion masses, giving rise to tree-level flavor violating couplings of the Higgs to fermions. The induced FCNCs are strongly constrained by various low energy experiments; if these constraints are somehow evaded, interesting signals at the LHC could also be generated.

The possibility of a flavor misalignment between the Higgs Yukawa matrices and the fermion mass matrices in the context of 5D warped scenarios was first briefly mentioned in [28], although it was not until [29] where a detailed analysis of the flavor structure of the couplings of the Higgs (brane localized) was first performed. There, the effects on the flavor violating Higgs couplings were found to be small (except for third generation quarks), with

the (hidden) assumption that the contribution from a specific type of operators is negligible. In a more general Higgs context (bulk or brane localized), all the sources of Higgs flavor violation were then pointed out in [11,30], including the previously neglected operators, although no analysis on the overall size of the Higgs FCNCs was performed. Moreover, in the limit of a brane localized Higgs, the effects of the larger sources of flavor are claimed to become negligible, and so it is again found that Higgs mediated FCNCs are highly suppressed in the case of a brane Higgs.

In this work, we show that the induced misalignment in the Higgs couplings is generically large and phenomenologically important in both bulk and brane localized Higgs scenarios. The main cause for this result is the effect of the originally neglected operators which, due to a subtlety in the treatment of the brane localized Higgs, ends up surviving in the brane limit and giving rise to important misalignments between the Higgs Yukawa couplings and the fermion mass matrices.

The outline of the paper is as follows: in Sec. II we review the model independent argument such that (TeV suppressed) higher order effective operators in the Higgs sector can lead to potentially large Higgs FCNCs. This is then applied to the 5D RS model, first in the mass insertion approximation in order to quickly estimate the size of the corrections. In Sec. III we proceed with a more precise calculation of the Higgs Yukawa couplings in the case of one fermion generation, and for a bulk Higgs scenario. The deviation in the Yukawa couplings is quite insensitive to how much the Higgs is localized near the IR brane; this result is confirmed in Sec. IV by doing a 5D computation for the case of an exactly IR localized Higgs field, and it seems at odds with the mass insertion approximation which suggests that the corrections to the flavor violating Higgs couplings should vanish in the brane Higgs limit. This apparent contradiction is addressed and resolved in that same section. In Sec. V we extend our results to the case of three generations and then in Sec. VI, we give an estimate of the expected overall size of the Yukawa coupling matrices. We also argue that the couplings of the Higgs to third generation fermions might be significantly suppressed. These estimates are confirmed in Sec. VII by the results of our numerical scan. Finally, Sec. VIII is devoted to the study of phenomenological implications of Higgs mediated flavor violations, where we discuss low energy bounds arising from $\Delta F = 2$ processes as well as interesting collider signatures.

II. FLAVOR MISALIGNMENT ESTIMATE

From an effective field theory approach it is easy to write the lowest order operators responsible for generating a misalignment in flavor space between the Higgs Yukawa couplings and the SM fermion masses. For simplicity we focus on the down-quark sector and write the following

dimension six operators of the four-dimensional (4D) effective Lagrangian [23–27]:

$$\lambda_{ij} \frac{H^2}{\Lambda^2} H \bar{Q}_{L_i} D_{R_j}, \quad k_{ij}^D \frac{H^2}{\Lambda^2} \bar{D}_{R_i} \not{D}_{R_j}, \quad \text{and} \quad k_{ij}^Q \frac{H^2}{\Lambda^2} \bar{Q}_{L_i} \not{Q}_{L_j} \quad (1)$$

where Q_{L_i} and D_{R_j} are the fermionic $SU(2)$ doublets and singlets of the SM, with λ_{ij} , k_{ij}^D , and k_{ij}^Q being complex coefficients and i, j are flavor indices; Λ is the cutoff or the threshold scale of the effective Lagrangian. Upon electroweak symmetry breaking (EWSB), these operators will give a correction to the fermion kinetic terms and to the fermion mass terms. Calling y_{ij} the original Yukawa couplings, the corrected fermion mass and kinetic terms become

$$\begin{aligned} & v_4 \left(y_{ij} + \lambda_{ij} \frac{v_4^2}{\Lambda^2} \right) \bar{Q}_{L_i} D_{R_j}, \\ & \left(\delta_{ij}/2 + k_{ij}^D \frac{v_4^2}{\Lambda^2} \right) \bar{D}_{R_i} \not{D}_{R_j}, \quad \text{and} \\ & \left(\delta_{ij}/2 + k_{ij}^Q \frac{v_4^2}{\Lambda^2} \right) \bar{Q}_{L_i} \not{Q}_{L_j}, \end{aligned} \quad (2)$$

where $v_4 = 174$ GeV is the Higgs electroweak vacuum expectation value (vev), i.e. $H = h/\sqrt{2} + v_4$, with h being the physical Higgs scalar. On the other hand, the induced operators involving two fermions and one physical Higgs h become:

$$\begin{aligned} & \left(y_{ij} + 3\lambda_{ij} \frac{v_4^2}{\Lambda^2} \right) \frac{h}{\sqrt{2}} \bar{Q}_{L_i} D_{R_j}, \\ & \left(2k_{ij}^D \frac{v_4}{\Lambda^2} \right) \frac{h}{\sqrt{2}} \bar{D}_{R_i} \not{D}_{R_j}, \quad \text{and} \\ & \left(2k_{ij}^Q \frac{v_4}{\Lambda^2} \right) \frac{h}{\sqrt{2}} \bar{Q}_{L_i} \not{Q}_{L_j}. \end{aligned} \quad (3)$$

From Eq. (2) it is clear that one has to redefine the fermion fields to canonically normalize the new kinetic terms and then perform a bi-unitary transformation to diagonalize the resulting mass matrix. These fermion redefinitions and rotations will not in general diagonalize the couplings from Eq. (3) and therefore, we will obtain tree-level flavor changing Higgs couplings, with a generic size controlled by $\frac{v_4^2}{\Lambda^2}$.

In the warped extra dimensions scenarios that we are interested in, we can estimate easily the size of this type of misalignments between the Higgs Yukawa couplings and the SM fermion masses by using the insertion approximation in KK language. The 5D spacetime we consider takes the usual Randall-Sundrum form [1]:

$$ds^2 = \frac{1}{(kz)^2} (\eta_{\mu\nu} dx^\mu dx^\nu - dz^2), \quad (4)$$

with the UV (IR) branes localized at $z = R$ ($z = R'$) and

with k being the curvature scale of the anti-de Sitter space. We are interested here in the flavor structure of the Yukawa couplings between the Higgs and the fermions. However, it is instructive to first consider the case of only one generation and study the (potentially large) corrections induced to the single Yukawa coupling. One can then easily generalize to three generations and find the misalignment between the fermion mass matrix and the Yukawa couplings matrix.

We will focus on the down-quark sector of a simple setup in which we consider the 5D fermions Q, D . They contain the 4D SM $SU(2)_L$ doublet and singlet fermions, respectively, with a 5D action

$$S_{\text{fermion}} = \int d^4x dz \sqrt{g} \left[\frac{i}{2} (\bar{Q} \Gamma^A \mathcal{D}_A Q - \mathcal{D}_A \bar{Q} \Gamma^A Q) + \frac{c_q}{R} \bar{Q} Q + (Q \rightarrow D) + (Y_d \bar{Q} H D + \text{H.c.}) \right] \quad (5)$$

where c_q and c_d are the 5D fermion mass coefficients and H is the bulk Higgs field localized towards IR brane. The wave functions of the fermion zero modes are determined by their corresponding 5D mass coefficients. To obtain a chiral spectrum, we choose the following boundary conditions for Q, D

$$Q_L(++), \quad Q_R(--), \quad D_L(--), \quad D_R(++). \quad (6)$$

Then, only Q_L and D_R will have zero modes, with wave functions

$$q_L^0(z) = f(c_q) \frac{R^{l-(1/2)+c_q}}{R^2} z^{2-c_q} \quad (7)$$

$$d_R^0(z) = f(-c_d) \frac{R^{l-(1/2)-c_d}}{R^2} z^{2+c_d}, \quad (8)$$

where we have defined $f(c) \equiv \sqrt{\frac{1-2c}{1-e^{1-2c}}}$ and the hierarchically small parameter $\epsilon = R/R' \approx 10^{-15}$, which is generally referred to as the ‘‘warp factor.’’ Thus, if we choose $c_q(-c_d) > 1/2$, then the zero modes wave functions are localized towards the UV brane; if $c_q(-c_d) < 1/2$, they are localized towards the IR brane. The wave functions of the KK modes are all localized near the IR brane. Note that the wave functions of the KK modes Q_R and D_L vanish at the IR brane due to their boundary conditions. The Yukawa couplings of the Higgs with fermions (zero modes or heavy KK modes) are set by the overlap integrals of the corresponding wave functions. For a bulk Higgs localized near the IR brane, the zero-zero-Higgs, zero-KK-Higgs, KK-KK-Higgs Yukawa couplings are given approximately by

$$Y_{d,00} \sim Y_* f(c_q) f(-c_d) \quad (9)$$

$$Y_{d,0n} \sim Y_* f(c_q) \quad \text{or} \quad Y_* f(-c_d) \quad (10)$$

$$Y_{d,nm} \sim Y_* \quad (11)$$

where $Y_* = Y_d/\sqrt{R}$ is the $O(1)$ dimensionless 5D Yukawa coupling, and we ignored $O(1)$ factors in the equations above. The SM fermions are mostly zero mode fermions with some small amount of mixing with KK mode fermions. Therefore, we can use the mass insertion approximation to calculate the masses and Yukawa couplings of SM fermions. This is shown in Fig. 1, where q_L^0, d_R^0 are zero modes of $SU(2)_L$ doublet and singlet fermions, respectively, and $q_L^{\text{KK}}, q_R^{\text{KK}}, d_L^{\text{KK}}, d_R^{\text{KK}}$ are KK mode fermions. From the Feynman diagram in Fig. 1 we see that the SM fermion mass is given by

$$m_{\text{SM}}^d \approx Y_{d,00} v_4 - Y_{d,0n} Y_{d,nm} Y_{d,m0} v_4 \frac{v^2}{M_{\text{KK}}^2} \approx f(c_q) Y_* f(-c_d) v_4 - f(c_q) \frac{Y_*^2 v_4^2}{M_{\text{KK}}^2} f(-c_d) Y_* v_4 \quad (12)$$

where v_4 is the Higgs vev and we assume that all KK fermion masses are of the same order (M_{KK}).

The 4D effective Yukawa couplings of SM fermions can be calculated using the same diagram. However in the second diagram of Fig. 1, we have to set two external H to their vev v_4 while the other one becomes the physical Higgs h , and there are three different ways to do this. Thus we obtain the 4D Yukawa couplings

$$y_{\text{SM}}^d \approx f(c_q) Y_* f(-c_d) - 3f(c_q) \frac{Y_*^2 v_4^2}{M_{\text{KK}}^2} f(-c_d) Y_* \quad (13)$$

We see that the SM fermion masses and the 4D Yukawa couplings are not universally proportional; indeed there is a shift with respect to the SM prediction of $m_{\text{SM}}^d = y_{\text{SM}}^d v_4$.

We thus define the shift Δ^d as

$$\Delta^d = m_{\text{SM}}^d - y_{\text{SM}}^d v_4 \quad (14)$$

and it is easy to see that the contribution of the diagrams of Fig. 1 to Δ^d is

$$\Delta_1^d \approx 2f(c_q) \frac{Y_*^2 v_4^2}{M_{\text{KK}}^2} f(-c_d) v_4 Y_*. \quad (15)$$

There is yet another source of shift between masses and Yukawa couplings coming this time from the corrections to the kinetic terms. This is the contribution which was pointed out and carefully computed in [29], and as we will see later, in agreement with our own results for that specific term. As shown in Fig. 2, the kinetic term for the fermion mode q_L^{SM} receives a correction induced by the

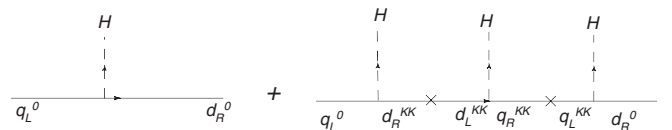


FIG. 1. Shift in masses and Yukawa couplings of SM fermions using the mass insertion approximation.

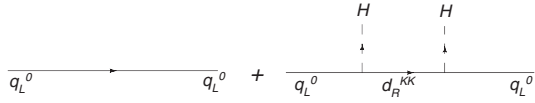


FIG. 2. Correction to kinetic terms using insertion approximation.

mixing with KK fermion modes

$$\begin{aligned} & \left(1 + Y_{d,0n} Y_{d,n0} \frac{H^2}{M_{\text{KK}}^2}\right) \bar{q}_L^{\text{SM}} i \not{\partial} q_L^{\text{SM}} \\ & \approx \left(1 + f(c_q)^2 \frac{(Y_* H)^2}{M_{\text{KK}}^2}\right) \bar{q}_L^{\text{SM}} i \not{\partial} q_L^{\text{SM}}. \end{aligned} \quad (16)$$

After redefining fields so that their kinetic term is canonical, there will be a new contribution to the shift between masses and Yukawa couplings given by

$$\Delta_2^d \approx f(c_q)^3 \frac{Y_*^2 v_4^2}{M_{\text{KK}}^2} f(-c_d) v_4 Y_*. \quad (17)$$

Similarly, the correction to the kinetic term of d_R^{SM} gives the contribution

$$\Delta_2^{d'} \approx f(c_q) \frac{Y_*^2 v_4^2}{M_{\text{KK}}^2} f(-c_d)^3 v_4 Y_*. \quad (18)$$

Adding all terms together, we find the total fermion mass-Yukawa shift

$$\begin{aligned} \Delta^d &= \Delta_1^d + \Delta_2^d + \Delta_2^{d'} \\ &\approx f(c_q) \frac{Y_*^2 v_4^2}{M_{\text{KK}}^2} f(-c_d) v_4 Y_* [2 + f(c_q)^2 + f(-c_d)^2]. \end{aligned} \quad (19)$$

If we extend to the case of three generations, we can see that this shift between SM fermion masses and Yukawa couplings produces a misalignment in flavor space between these. This misalignment will lead to flavor violating Higgs couplings once the fermion mass matrix is diagonalized.

For the first two generation quarks, we need $f(c_q)$, $f(-c_d) \ll 1$ to reproduce their small masses. Therefore, for these first two generations, the shift coming from the correction to kinetic terms (Fig. 2) is negligible and the correction coming from the diagrams in Fig. 1 will dominate. However, for the third generation, all effects are comparable. It is interesting to point out that the expression [Eq. (19)] (valid for one generation) is always positive, which leads to a reduction in the 4D effective Yukawa couplings compared to the SM ones.

A. Brane Higgs subtlety

Finally, we must mention that there is a subtlety in the case of an exactly brane localized Higgs. As pointed out in [11,30], since the wave functions of q_R^{KK} and d_L^{KK} vanish at

TeV brane (due to Dirichlet boundary conditions), their couplings to a brane localized Higgs should also vanish. This means that the second diagram in Fig. 1 should give no contribution to the fermion mass-Yukawa shift (or at best a highly suppressed one). We would then expect to be left with only the correction coming from the kinetic term (Fig. 2), which as stated above is negligible for light quarks. We observe, however, that upon EWSB, the wave functions q_R^{KK} and d_L^{KK} become discontinuous at the brane location [31], with the jump of the wave functions being proportional to the brane Higgs vev v_4 . This discontinuity requires some sort of regularization of the brane location, meaning that the couplings of q_R^{KK} and d_L^{KK} with the brane Higgs would be infinitesimally small, but nonzero. But we note that in the second diagram of Fig. 1, one has to sum over infinite KK modes and even though each KK mode will give an infinitesimally small contribution, the sum of infinite terms can lead to a finite (nonzero) result (and as it turns out, this is what happens, as shown explicitly in Appendix C for this mass insertion approximation).

This brane Higgs issue is avoided in [29] because the authors did not include in their brane action any operator of the type $H Q_R D_L$. By avoiding these, the contribution to the shift Δ^d coming from the diagrams of Fig. 1 is simply not present (except for highly suppressed corrections of order $\frac{v_4^2 m_f^2}{M_{\text{KK}}^2}$ which are safe to ignore).

We will address thoroughly this issue in the next two sections and again in Appendix C, since we do find that the flavor misalignment produced by the diagrams of Fig. 1 is large and of the same order for both bulk Higgs and brane Higgs scenarios.

III. 5D CALCULATION: BULK HIGGS SCENARIO

In this section we perform a 5D calculation in order to evaluate more precisely the shift between Yukawa couplings and masses of SM fermions. We start by working with a single fermion generation for clarity but will later extend our results to the three generations case.

To proceed, we will need to solve for the wave functions of SM fermions along the fifth dimension in the bulk Higgs [32,33] scenario. This corresponds to including the contribution of all KK modes of the mass insertion approximation, and not just the lightest ones. As we will see, the most important shift does not go away as we push the Higgs profile towards the IR brane. In the bulk Higgs scenario, the Higgs comes from a 5D scalar with the following action :

$$\begin{aligned} \mathcal{L}_{\text{Higgs}} &= \int dz d^4 x \left(\frac{R}{z}\right)^3 \left[\text{Tr} |D_M H|^2 - \frac{\mu^2}{z^2} \text{Tr} |H|^2 \right] \\ &\quad - V_{\text{UV}}(H) \delta(z - R) - V_{\text{IR}}(H) \delta(z - R') \end{aligned} \quad (20)$$

where μ is the 5D mass for Higgs in unit of k . The

boundary potentials $V_{UV}(H)$ and $V_{IR}(H)$ give the boundary conditions for the Higgs wave function. We can choose these boundary conditions such that the profile of the Higgs vev takes the simple form

$$v(z) = V(\beta)z^{2+\beta} \quad (21)$$

where $\beta = \sqrt{4 + \mu^2}$ and

$$V(\beta) = \sqrt{\frac{2(1 + \beta)}{R^3(1 - (R'/R)^{2+2\beta})}} \frac{v_4}{(R')^{1+\beta}} \quad (22)$$

where v_4 is the SM Higgs vev. This nontrivial vev $v(z)$ is localized towards the IR brane solving the Planck-weak hierarchy problem. Nevertheless we will treat the brane Higgs case separately later to review possible subtleties inherent to its localization by a Dirac delta function.

After writing the 5D fermions in two component notation,

$$Q = \begin{pmatrix} Q_L \\ Q_R \end{pmatrix}$$

and

$$D = \begin{pmatrix} D_L \\ D_R \end{pmatrix},$$

we perform a ‘‘mixed’’ KK decomposition as

$$Q_L(x, z) = q_L(z)Q_L(x) + \dots \quad (23)$$

$$Q_R(x, z) = q_R(z)Q_R(x) + \dots \quad (24)$$

$$D_L(x, z) = d_L(z)D_L(x) + \dots \quad (25)$$

$$D_R(x, z) = d_R(z)D_R(x) + \dots \quad (26)$$

where $Q_L(x)$, $D_R(x)$ correspond to the light 4D SM fermions and the ‘‘...’’ include the rest of heavy KK fermion fields. $q_{L,R}(z)$, $d_{L,R}(z)$ are the corresponding profiles of the 4D SM fermions $Q_L(x)$ and $D_R(x)$ which verify the Dirac equation

$$-i\bar{\sigma}^\mu \partial_\mu Q_L(x) + m_d D_R(x) = 0, \quad (27)$$

$$-i\sigma^\mu \partial_\mu D_R(x) + m_d^* Q_L(x) = 0, \quad (28)$$

with m_d being the 4D SM down-type quark mass (the analysis can be carried out for up-type quarks in similar fashion).

The four profiles $q_{L,R}(z)$ and $d_{L,R}(z)$ must verify the coupled equations coming from the equations of motion.

$$-m_d q_L - q'_R + \frac{c_q + 2}{z} q_R + \left(\frac{R}{z}\right) v(z) Y_d d_R = 0 \quad (29)$$

$$-m_d^* q_R + q'_L + \frac{c_q - 2}{z} q_L + \left(\frac{R}{z}\right) v(z) Y_d d_L = 0 \quad (30)$$

$$-m_d d_L - d'_R + \frac{c_d + 2}{z} d_R + \left(\frac{R}{z}\right) v(z) Y_d^* q_R = 0 \quad (31)$$

$$-m_d^* d_R + d'_L + \frac{c_d - 2}{z} d_L + \left(\frac{R}{z}\right) v(z) Y_d^* q_L = 0 \quad (32)$$

where the $'$ denotes derivative with respect to the extra coordinate z and $[Y_d] = -1/2$ is the 5D Yukawa coupling. Even if one knows the analytical form of the nontrivial Higgs vev $v(z)$, solving analytically this system of equations might still be quite hard. Nevertheless it is simple to find the misalignment between Higgs Yukawa couplings and fermion masses based on the previous equations. To proceed, let us first multiply Eq. (29) by $q_L^*(z)$ and the conjugate of Eq. (30) by $q_R(z)$, and then subtract them. One obtains

$$m_d(|q_L|^2 - |q_R|^2) + z^4 \left(\frac{q_L^* q_R}{z^4}\right)' - \left(\frac{R}{z}\right) v(z) (Y_d d_R q_L^* - Y_d^* q_R d_L^*) = 0. \quad (33)$$

We can now multiply by $\frac{R^4}{z^4}$ and integrate the whole expression between $z = R$ and $z = R'$ and obtain

$$R^4 \int_R^{R'} dz \left(\frac{m_d}{z^4} (|q_L|^2 - |q_R|^2) - \frac{Rv(z)}{z^5} (Y_d d_R q_L^* - Y_d^* q_R d_L^*) \right) + \left(q_L^* q_R \frac{R^4}{z^4} \right) \Big|_R^{R'} = 0. \quad (34)$$

The boundary conditions for the profile $q_R(z)$ are chosen to be Dirichlet at both boundaries, i.e. $q_R(R) = q_R(R') = 0$, which means that the last term of Eq. (34) identically vanishes. Moreover, canonical normalization of the SM d quark imposes the extra constraint

$$R^4 \int_R^{R'} \frac{dz}{z^4} (|q_L|^2 + |d_L|^2) = 1. \quad (35)$$

We can therefore rewrite Eq. (34) as

$$m_d = R^4 \int_R^{R'} dz \left(\frac{m_d}{z^4} (|d_L|^2 + |q_R|^2) + \frac{Rv(z)}{z^5} (Y_d d_R q_L^* - Y_d^* q_R d_L^*) \right) \quad (36)$$

Note that this identity is exact, but also that each profile $q_{R,L}(z)$ and $d_{R,L}(z)$ depend on the mass m_d . In the zero mode approximation, the profiles with Dirichlet boundary conditions, $q_R^0(z)$ and $d_L^0(z)$ vanish, and the identity can be expressed as

$$m_d \simeq m_d^0 = R^5 \int_R^{R'} dz \frac{v(z)}{z^5} Y_d d_R^0 q_L^{0*} \quad (37)$$

which agrees with the intuition that fermion mass is mostly generated by the 5D Yukawa couplings between the 5D

Higgs and the zero mode fermion profiles. From the action in Eq. (5) we also extract the 4D Yukawa coupling of the Higgs field (the lightest KK mode of the 5D Higgs) and the SM down-type quark.

$$y_4^d = R^5 \int_R^{R'} dz \frac{h(z)}{z^5} (Y_d d_R q_L^* + Y_d^* q_R d_L^*) \quad (38)$$

where $h(z)$ is the profile of the physical Higgs field. It is easy to show that the Higgs vev solution $v(z)$ is related to the profile of the physical light Higgs $h(z)$ (lightest KK mode) by

$$h(z) = \frac{v(z)}{v_4} \left(1 + \mathcal{O}\left(\frac{m_h^2 z^2}{1 + \beta}\right) \right) \quad (39)$$

so for a light enough Higgs field both profiles $h(z)$ and $v(z)$ are proportional to each other. For a moderately heavy physical Higgs, there will be a misalignment between the profiles of the Higgs vev and the physical Higgs, leading to a misalignment between fermion masses and Yukawa couplings. However, this effect can actually be decoupled if the Higgs is pushed towards the IR brane (by increasing the parameter β). In this case, the Higgs vev profile will be more and more aligned with that of the physical Higgs, so that they become identical in the brane Higgs limit. This source of Higgs flavor violating couplings will be controlled by the parameter $\frac{1}{\beta+1}$ and for the sake of clarity we will ignore its effects in the rest of the paper because, as we discuss in Appendix B, they are numerically small and can be decoupled by pushing the Higgs towards the IR brane.

We can then compute the shift $\Delta^d = m_d - v_4 y_4^d$ between the fermion mass m_d and the Yukawa coupling y_4^d as

$$\Delta^d = R^4 \int_R^{R'} dz \left(\frac{m_d}{z^4} (|d_L|^2 + |q_R|^2) - 2Y_d^* \frac{Rv(z)}{z^5} q_R d_L^* \right). \quad (40)$$

This identity shows that the shift has to be relatively small since it vanishes in the zero mode approximation.

To proceed further, we will use a perturbative approach such that we assume that $(v_4 R') \ll 1$ where v_4 is the SM Higgs vev. Thus, once we know the analytical form of the vev profile $v(z)$ [see Eq. (21)] we can solve perturbatively the system of coupled Eqs. (29)–(32).¹

We find

$$q_L(z) = Q_L z^{2-c_q} [1 + \mathcal{O}(v_4^2 R'^2)] \quad (41)$$

$$d_R(z) = D_R z^{2+c_d} [1 + \mathcal{O}(v_4^2 R'^2)] \quad (42)$$

and

¹It would be interesting to use this perturbative technique in the context of fermion flavor in soft-wall scenarios [34–36] given that the setup is quite similar; we will leave this analysis for future studies.

$$q_R(z) = \left[m_d Q_L \left(\frac{R^{1-2c_q}}{1-2c_q} z^{2+c_q} - \frac{1}{1-2c_q} z^{3-c_q} \right) + Y_d \frac{RV(\beta)}{(2+\beta-c_q+c_d)} D_R z^{4+\beta+c_d} \right] \times [1 + \mathcal{O}(v_4^2 R'^2)] \quad (43)$$

$$d_L(z) = \left[m_d^* D_R \left(-\frac{R^{1+2c_d}}{1+2c_d} z^{2-c_d} + \frac{1}{1+2c_d} z^{3+c_d} \right) - Y_d^* \frac{RV(\beta)}{(2+\beta-c_q+c_d)} Q_L z^{4+\beta-c_q} \right] \times [1 + \mathcal{O}(v_4^2 R'^2)] \quad (44)$$

with the constants Q_L and D_R fixed by canonical normalization of the kinetic terms giving

$$Q_L = \sqrt{\frac{1-2c_q}{\epsilon^{2c_q-1} - 1}} R^{c_q-5/2} \quad (45)$$

$$D_R = \sqrt{\frac{1+2c_d}{\epsilon^{-2c_d-1} - 1}} R^{-c_d-5/2}. \quad (46)$$

Equipped with the solutions from Eqs. (41) to (44) one can evaluate perturbatively the shift Δ^d defined in Eq. (40). For simplicity, we present here the results for UV localized fermions ($c_q > 0.5$, $c_d < -0.5$). The general results for both UV and IR localized fermions are presented in Appendix A. We find that the main contribution to the shift coming from the last term in Eq. (40) can be written as

$$\Delta_1^d = 2|m_d|^2 m_d R'^2 \left[\frac{(2+\beta+c_d-c_q)}{(6+3\beta+c_d-c_q)} - 2 \frac{(2+\beta+c_d-c_q)}{(2\beta+4)} + \frac{(2+\beta+c_d-c_q)}{(2+\beta+c_q-c_d)} \right] \times \frac{1}{f(c_q)^2 f(-c_d)^2}. \quad (47)$$

This result corresponds to the one we estimated earlier by using the insertion approximation [see Eq. (15)].

The first term in Eq. (40) gives a subleading contribution to the shift

$$\Delta_2^d = m_d |m_d|^2 R'^2 \left[\frac{1}{f(c_q)^2} \left(\frac{2c_q-1}{2c_q+1} + \frac{1}{5+2\beta+2c_d} - \frac{1}{3+c_q+c_d+\beta} \right) + (c_{q,d} \rightarrow -c_{d,q}) \right] \quad (48)$$

which corresponds to the one coming from the kinetic correction using the insertion approximation [Eq. (17) and (18)].

Even if the fermion mass m_d is small, the large warp factor $\frac{1}{f(c_q)^2 f(-c_d)^2} \approx \epsilon^{2-2c_q+2c_d}$ will overcome most of the

suppression, rendering the shift to be of the order $\Delta^d \sim m_d v_4^2 R^2$. The shift is generally on the percent level with respect to fermion masses, but a misalignment of this order in the Higgs Yukawa couplings should introduce strong constraints due to FCNCs.

A. Pushing the Higgs from the bulk to the brane

Note that in the $\beta \rightarrow \infty$ limit, the profile of the Higgs vev tends to become brane localized, as well as the light physical Higgs and the rest of Higgs KK modes. In this limit, the shift Δ_1^d produced between the fermion mass and the Yukawa coupling, coming from the diagrams of Fig. 1, reduces to

$$\Delta_1^d = \frac{2}{3} |m_d|^2 m_d R^2 \frac{1}{f(c_q)^2 f(-c_d)^2}, \quad (49)$$

and, in particular, we see that the effect does not decouple (i.e. it is nonzero). The fact that the expected misalignment is more or less independent on the localization of the Higgs is one of our main results since the bounds and predictions that we will extract can then be considered a general feature of RS models with fields in the bulk (and a Higgs scalar localized near or at IR brane).² The shift Δ_2^d coming from the corrections to the fermion kinetic terms (Fig. 2) becomes in the $\beta \rightarrow \infty$ limit

$$\begin{aligned} \Delta_2^d = m_d |m_d|^2 R^2 & \left[\frac{1}{f(c_q)^2} \left(\frac{2c_q - 1}{2c_q + 1} \right) + \frac{1}{f(-c_d)^2} \right. \\ & \left. \times \left(\frac{2c_d + 1}{2c_d - 1} \right) \right], \end{aligned} \quad (50)$$

in agreement with the results found in [29] (for a brane Higgs scenario).

Maybe it can be useful to discuss the validity of the $\beta \rightarrow \infty$ limit starting from a bulk Higgs scenario. Let us first look at the mass spectrum in this case. The Higgs profile is given by Eq. (B1) and to find its mass eigenvalues one has to satisfy the appropriate boundary conditions at the IR brane [32]

$$\partial_z h + \left(\frac{R'}{R} \right) m_{\text{TeV}} h \Big|_{R'} = 0. \quad (51)$$

This will lead to one light mode (i.e. SM Higgs) and a tower of heavy modes with masses proportional to $\sim \beta/R'$, and so in the $\beta \rightarrow \infty$ limit all the KK Higgs excitations are decoupled from the low energy spectrum. This means that in this limit we can treat Higgs field as an effective four-dimensional field, and thus it corresponds to the brane Higgs scenario. As mentioned earlier (and in Appendix B), the misalignment caused by a difference in

²An interesting exception to these results in the Higgs sector, proposed in [23], would be to eliminate the Higgs as a fundamental scalar and consider the fifth component of a gauge field as playing the Higgs role in EWSB.

profiles between the Higgs physical field and its vev (and which we have neglected) will also disappear, as one can interpret that specific misalignment as a result of the mixing between SM Higgs and the heavy Higgs KK modes, which is controlled by $\frac{1}{\beta} \sim \frac{1}{M_{\text{KK}}^{\text{Higgs}} R'}$.

Let us now look on the couplings of fermions to the Higgs in this limit. For the zero modes we will get

$$y_d^{\text{SM}} = \frac{\sqrt{2(1+\beta)}}{(2-c_q+c_d+\beta)} \frac{Y_d}{\sqrt{R}} f(c_q) f(-c_d) \quad (52)$$

where $[y_d^{\text{SM}}] = 0$, $[Y_d] = -1/2$; similarly one can look at the couplings of two KK fermions to the Higgs and in this case one finds its dependence to be $\sim \frac{1}{\sqrt{\beta}} \frac{Y_d}{\sqrt{R}}$. Naively both couplings do vanish in the $\beta \rightarrow \infty$ limit. But if the 5D couplings Y_d scale as $\sqrt{\beta}$ then these couplings will have a finite limit given by the usual brane Higgs results. One can argue whether we can scale the 5D Yukawas as $\sqrt{\beta}$ because such large Yukawas should violate perturbativity of the theory, but as was shown above the couplings of the Higgs to the KK fermions are still $O(1)$. One can see that only the KK excitations of the Higgs will have couplings with KK fermions $\sim Y_d R^{-1/2} \propto O(\sqrt{\beta})$, but their masses are $O(\frac{\beta}{R'})$ and they are completely decoupled from the spectrum. So we conclude this discussion by stressing that it is consistent to consider the limit $\beta \rightarrow \infty$ with $Y_d \propto \sqrt{\beta}$ and it coincides with the usual brane Higgs scenario.

IV. 5D CALCULATION: BRANE HIGGS SCENARIO

We argued in Sec. II that one might expect that the major contribution to the misalignment Δ_1^d vanishes in the brane Higgs case since the odd KK modes $q_R^{\text{KK}}, d_L^{\text{KK}}$ have vanishing wave functions on the IR brane. We also briefly mentioned that in the mass insertion approximation, one actually might need to sum the infinite tower of fermion KK modes to obtain a nonvanishing contribution (see Appendix C for details). However, without invoking that explanation, we just saw that in the $\beta \rightarrow \infty$ limit, Δ_1^d approaches a nonzero value of same numerical order as the $\beta = \text{finite}$ case. Since the $\beta \rightarrow \infty$ limit of bulk Higgs corresponds to a brane localized Higgs, there seems to be a counterintuitive subtlety. In this section we try to address and resolve this point in a more precise way, by performing the 5D calculation of the shift Δ_1^d for the specific scenario of a brane Higgs.

For brane Higgs, we can write the Yukawa couplings in the Lagrangian as

$$\begin{aligned} S_{\text{brane}} = \int d^4 x dz \delta(z - R') & \left(\frac{R}{z} \right)^4 H (Y_1^{5D} R \bar{Q}_L \mathcal{D}_R \\ & + Y_2^{5D} R \bar{Q}_R \mathcal{D}_L + \text{H.c.}). \end{aligned} \quad (53)$$

Here we choose the convention with $\dim[Y_{1,2}^{5D}] = 0$. Note that compared to the bulk Higgs case, the Yukawa cou-

plings Y_1^{5D} and Y_2^{5D} are independent and both $\sim O(1)$. However, they should be of the same order due to the philosophy of flavor anarchy and naturalness. We can do KK decomposition as before, then the equations satisfied by the wave functions are

$$-m_d q_L - \partial_z q_R + \frac{c_q + 2}{z} q_R + v_4 \delta(z - R') Y_1^{5D} R' d_R = 0 \quad (54)$$

$$-m_d^* q_R + \partial_z q_L + \frac{c_q - 2}{z} q_L + v_4 \delta(z - R') Y_2^{5D} R' d_L = 0 \quad (55)$$

$$-m_d d_L - \partial_z d_R + \frac{c_u + 2}{z} d_R + v_4 \delta(z - R') Y_2^{5D*} R' q_R = 0 \quad (56)$$

$$-m_d^* d_R + \partial_z d_L + \frac{c_u - 2}{z} d_L + v_4 \delta(z - R') Y_1^{5D*} R' q_L = 0. \quad (57)$$

Notice that the odd wave functions q_R and d_L vanish at the IR brane. But the delta functions in equations above give a jump for q_R and d_L at the IR brane, which makes their values at IR brane ambiguous [31]. To remove this ambiguity, we ‘‘regularize’’ the delta in the following way:

$$\delta(z - R') = \lim_{\varepsilon \rightarrow 0} \begin{cases} \frac{1}{\varepsilon}, & R' - \varepsilon < z < R' \\ 0, & z < R' - \varepsilon. \end{cases} \quad (58)$$

This regularization is in a way similar to treating the Higgs as a bulk field and then taking the limit $\beta \rightarrow \infty$, although without apparent divergences coming from taking β to be large. In any case one could also perform other regularization methods to remove the wave function ambiguities at the IR brane.³

Now we can easily impose Dirichlet boundary conditions for the q_R, d_L profiles at IR brane

$$q_R(R') = d_L(R') = 0 \quad (60)$$

³For example, we could have chosen instead to move the delta function location from R' to $(R' - \varepsilon)$, and enforce the usual boundary conditions on the fields at $z = R'$. Then, at the very end, we would take the limit $\varepsilon \rightarrow 0$ [31]. In that case we find

$$d_L(z), q_R(z) \propto v_4 Y_1^{5D} \theta(z - R' + \varepsilon) \quad \text{for } R' - 2\varepsilon < z < R', \quad (59)$$

where we have used the step function $\theta(x) = 1$ for $x < 1$ and $\theta(x) = 0$ for $x > 0$. Inserting this into Eq. (40) we obtain the same misalignment as in Eq. (65), namely,

$$\begin{aligned} \Delta_1^d &\propto 2(v_4 R')^3 (Y_1^{5D})^2 Y_2^{5D*} \int_{R'-2\varepsilon}^{R'} dz \delta(z - R' + \varepsilon) \\ &\times [\theta(z - R' + \varepsilon)]^2 \propto \frac{2}{3} (v_4 R')^3 (Y_1^{5D})^2 Y_2^{5D*}. \end{aligned}$$

Integrating equations of motion [Eq. (54)] from $(R' - \varepsilon < z < R')$ will lead to

$$q_R(R') - q_R(R' - \varepsilon) = v_4 Y_1^{5D} R' d_R(R') \quad (61)$$

$$d_L(R') - d_L(R' - \varepsilon) = -v_4 Y_1^{5D*} R' q_L(R'). \quad (62)$$

For the rectangular potential profiles q_R, d_L will drop to zero linearly in the region $R' - \varepsilon < z < R'$, so the profiles near the IR brane can be approximated by

$$q_R(z) = v_4 Y_1^{5D} R' d_R(R') \left(\frac{z - R'}{\varepsilon} \right) \quad \text{for } R' - \varepsilon < z < R', \quad (63)$$

$$\begin{aligned} d_L(z) &= -v_4 Y_1^{5D*} R' q_L(R') \left(\frac{z - R'}{\varepsilon} \right) \\ &\text{for } R' - \varepsilon < z < R'. \end{aligned} \quad (64)$$

From our previous discussion, the main contribution to the misalignment between SM fermion masses and Yukawa couplings come from the second term of Eq. (40), so plugging in the odd wave functions from Eq. (63), we get

$$\begin{aligned} \Delta_1^d &= 2(Y_2^{5D})^* (Y_1^{5D})^2 R'^3 v_4^3 d_R(R') q_L^*(R') \left(\frac{R}{R'} \right)^4 \\ &\times \int_{R'-\varepsilon}^{R'} dz \frac{1}{\varepsilon} \left(\frac{z - R'}{\varepsilon} \right)^2 \\ &= \frac{2}{3} (Y_2^{5D})^* (Y_1^{5D})^2 R'^3 v_4^3 d_R(R') q_L^*(R') \left(\frac{R}{R'} \right)^4. \end{aligned} \quad (65)$$

On the other hand, to leading order in Higgs vev, the SM fermion mass is given by

$$m_d \approx \left(\frac{R}{R'} \right)^4 v_4 Y_1^{5D} R' q_L^*(R') d_R(R'). \quad (66)$$

Therefore, the misalignment can be expressed as

$$\begin{aligned} \Delta_1^d &= \frac{2}{3} m_d Y_1^{5D} (Y_2^{5D})^* v_4^2 R'^2 \\ &= \frac{2}{3} |m_d|^2 m_d R'^2 \left(\frac{Y_2^{5D}}{Y_1^{5D}} \right)^* \frac{1}{f(c_q)^2 f(-c_d)^2}. \end{aligned} \quad (67)$$

As advertised before, this result agrees with the one obtained in the previous section for the bulk Higgs scenario, once we take $\beta \rightarrow \infty$ [Eq. (47)]. We again stress that this result shows that upon careful derivation, the misalignment obtained does not vanish in the particular case of a Brane localized Higgs. The main difference though, is the appearance of the independent couplings Y_2^{5D} , which in the bulk Higgs case are forced to be equal to Y_1^{5D} by 5D general covariance. These couplings Y_2^{5D} are not necessary for generating fermion masses, and so it is technically possible to set their values as small as necessary to suppress the obtained misalignment. Nevertheless this seems to go against the main philosophy of our approach which is to

assume the value of all dimensionless 5D parameters of order one.

Again, the fact that Δ_1^d is nonzero in the brane Higgs case is hard to understand in the mass insertion approximation since the contribution from each KK fermion (see Fig. 1) seems to be vanishing. In Appendix C we show that to resolve this point we need to sum up all the KK modes of the mass insertion approximation, as already mentioned before.

The subleading contribution to the misalignment between SM fermion masses and Yukawa coupling can be calculated in a similar way as in the previous section, and the result is (for UV localized fermions)

$$\Delta_2^d = m_d |Y_1^{5D}|^2 v_4^2 R^2 \left[f(-c_d)^2 \frac{2c_q - 1}{2c_q + 1} + (c_{q,d} \rightarrow -c_{d,q}) \right] \quad (68)$$

$$= m_d |m_d|^2 R^2 \left[\frac{1}{f(c_q)^2} \left(\frac{2c_q - 1}{2c_q + 1} \right) + (c_{q,d} \rightarrow -c_{d,q}) \right]. \quad (69)$$

We can see that for the first two generations, we have $\Delta_2^d \ll \Delta_1^d$, and it agrees with Eq. (48) in the $\beta \rightarrow \infty$ limit. The result for both UV and IR localized fermions is given by

$$\Delta_2^d = m_d |m_d|^2 R^2 [K(c_q) + K(-c_d)] \quad (70)$$

with

$$K(c) \equiv \frac{1}{1-2c} \left[-\frac{1}{\epsilon^{2c-1} - 1} + \frac{\epsilon^{2c-1} - \epsilon^2}{(\epsilon^{2c-1} - 1)(3-2c)} + \frac{\epsilon^{1-2c} - \epsilon^2}{(1+2c)(\epsilon^{2c-1} - 1)} \right]. \quad (71)$$

One can see that Δ_1^d and Δ_2^d can be of the same order only for IR localized fermions.

V. GENERALIZING TO THREE GENERATIONS

We can generalize the calculations presented in the Secs. III and IV to 3 generations. For simplicity we perform the analysis in the brane Higgs scenario here. To leading order in Yukawa, the SM fermion mass matrix is

$$\hat{m}_{\alpha\beta}^d = [\hat{F}_q \hat{Y}_1^{5D} \hat{F}_d]_{\alpha\beta} v_4 \quad (72)$$

where \hat{m} means a 3×3 matrix in flavor space and $\hat{F}_{q,d} = \text{diag}[f(c_{q_i}, c_{d_i})]$. Using the same technique as before, we can easily show that the misalignment between fermion mass and Yukawa coupling matrix is $\hat{\Delta}^d = \hat{\Delta}_1^d + \hat{\Delta}_2^d$, with

$$\hat{\Delta}_{1,\alpha\beta}^d = \frac{2}{3} [\hat{F}_q \hat{Y}_1^{5D} (\hat{Y}_2^{5D})^\dagger \hat{Y}_1^{5D} \hat{F}_d]_{\alpha\beta} (v_4^3 R^2) \quad (73)$$

$$= \frac{2}{3} \left[\hat{m}^d \frac{1}{\hat{F}_d} (\hat{Y}_2^{5D})^\dagger \frac{1}{\hat{F}_q} \hat{m}^d \right]_{\alpha\beta} (v_4^3 R^2) \quad (74)$$

and

$$\hat{\Delta}_{2,\alpha\beta}^d = [\hat{m}^d (\hat{m}^{d\dagger} \hat{K}(c_q) + \hat{K}(-c_d) \hat{m}^{d\dagger}) \hat{m}^d]_{\alpha\beta} R^2. \quad (75)$$

The subdominant contribution here [Eq. (75)] agrees with the result found in [29]. The crucial observation is that $\hat{m}_{\alpha\beta}^d$ and $\hat{\Delta}_{\alpha\beta}^d$ are generally not aligned in flavor space. Thus when we diagonalize the quark mass matrix with a bi-unitary transformation $\hat{m}^d \rightarrow O_{d_L}^\dagger \hat{m}^d O_{d_R}$, the Yukawa couplings will not be diagonal. To be more specific, in models of flavor anarchy, we have

$$(O_{d_L, d_R})_{\alpha\beta} \sim \frac{F_{q_\alpha, d_\alpha}}{F_{q_\beta, d_\beta}} \quad \text{for } \alpha < \beta. \quad (76)$$

Then the off-diagonal Yukawa coupling will be [dominated by Eq. (73)]

$$\hat{Y}_{\alpha\beta}^{\text{off}} = -(O_{d_L}^\dagger \hat{\Delta}^d O_{d_R})_{\alpha\beta} \frac{1}{v_4} \sim \frac{2}{3} F_{q_\alpha} \bar{Y}^3 F_{d_\beta} v_4^2 R^2 \quad (77)$$

where \bar{Y} is the typical value of the dimensionless 5D Yukawa coupling.

VI. ESTIMATES OF HIGGS FCNC IN FLAVOR ANARCHY

In this section, we estimate the off-diagonal couplings of Higgs to SM fermions (assuming again for simplicity a brane Higgs scenario). And then we do a numerical scan over anarchical Yukawa couplings to support our estimates. We first parametrize the Higgs Yukawa couplings as

$$\mathcal{L}_{\text{HFV}} = a_{ij}^d \sqrt{\frac{m_i^d m_j^d}{v_4^2}} H \bar{d}_L^i d_R^j + \text{H.c.} + (d \leftrightarrow u). \quad (78)$$

We can use Eq. (76) and (77) to estimate the sizes of $a_{ij}^{u,d}$. For example, we have

$$\begin{aligned} a_{12}^d &\sim \frac{2}{3} F_{q_1} \bar{Y}^3 F_{d_2} v^2 R^2 \sqrt{\frac{v_4^2}{m_s m_d}} \\ &= \frac{2}{3} \frac{F_{q_1}}{F_{q_2}} \bar{Y}^2 v_4 R^2 F_{q_2} \bar{Y} v_4 F_{d_2} \sqrt{\frac{v_4^2}{m_s m_d}} \sim \frac{2}{3} \lambda \bar{Y}^2 v_4^2 R^2 \sqrt{\frac{m_s}{m_d}}, \end{aligned} \quad (79)$$

where $\lambda \approx 0.22$ is the Wolfenstein parameter, and we used $F_{q_1}/F_{q_2} \sim (O_{d_L})_{12} \sim (V_{\text{CKM}})_{12} \sim \lambda$. We can find the other $a_{ij}^{u,d}$'s in similar fashion. Here we present our results from estimates:

$$a_{ij}^d \sim \delta_{ij} - \frac{2}{3} \bar{Y}^2 v_4^2 R^2 \begin{pmatrix} 1 & \lambda \sqrt{\frac{m_s}{m_d}} & \lambda^3 \sqrt{\frac{m_b}{m_d}} \\ \frac{1}{\lambda} \sqrt{\frac{m_d}{m_s}} & 1 & \lambda^2 \sqrt{\frac{m_b}{m_s}} \\ \frac{1}{\lambda^3} \sqrt{\frac{m_d}{m_b}} & \frac{1}{\lambda^2} \sqrt{\frac{m_s}{m_b}} & 1 \end{pmatrix} \quad (80)$$

$$a_{ij}^u \sim \delta_{ij} - \frac{2}{3} \bar{Y}^2 v_4^2 R^2 \begin{pmatrix} 1 & \lambda \sqrt{\frac{m_c}{m_u}} & \lambda^3 \sqrt{\frac{m_t}{m_u}} \\ \frac{1}{\lambda} \sqrt{\frac{m_u}{m_c}} & 1 & \lambda^2 \sqrt{\frac{m_t}{m_c}} \\ \frac{1}{\lambda^3} \sqrt{\frac{m_u}{m_t}} & \frac{1}{\lambda^2} \sqrt{\frac{m_c}{m_t}} & 1 \end{pmatrix}. \quad (81)$$

Note that the results we presented here are just estimates for the size of $a_{ij}^{u,d}$, not their signs or phases. However, for the third generation quarks, the corrections almost always suppress the Yukawa couplings if $Y_1 = Y_2$ (which is natural in bulk Higgs scenario) and are typically larger than the previous estimates. We argue this point in the next subsection.

A. Yukawa couplings of the third generation when $Y_1 = Y_2$

We can obtain a better estimate on the typical size of the diagonal entries of the Yukawa coupling matrices by going back to Eq. (74) and assume that $Y_1 = Y_2$. Its form simplifies further to

$$\hat{\Delta}_{1,\alpha\beta}^u = \frac{2}{3} R^2 \left[\hat{m}^u \frac{1}{\hat{F}_u^2} (\hat{m}^u)^\dagger \frac{1}{\hat{F}_q^2} \hat{m}^u \right]_{\alpha\beta} \quad (82)$$

where we have written the misalignment in the up-sector. Now we perform the bi-unitary rotation needed to go to the physical fermion basis, and study the element (33) of the overall Yukawa coupling, i.e.

$$\begin{aligned} a_{ii} - 1 &= -\frac{2R^2}{3m_i} \left[O_{u_L}^\dagger \hat{m}^u \frac{1}{\hat{F}_u^2} \hat{m}^{u\dagger} \frac{1}{\hat{F}_q^2} \hat{m}^u O_{u_R} \right]_{33} \\ &= -\frac{2R^2}{3m_i} (m_u^{\text{diag}})_{33} \left(O_{u_R}^\dagger \frac{1}{\hat{F}_u^2} O_{u_R} \right)_{3j} (m_u^{\text{diag}})_{jj} \\ &\quad \times \left(O_{u_L}^\dagger \frac{1}{\hat{F}_q^2} O_{u_L} \right)_{j3} (m_u^{\text{diag}})_{33}. \end{aligned} \quad (83)$$

First let us look at the contribution to a_{ii} when the “ j ” index is equal to 3 (i.e. in the middle mass matrix m_u^{diag} we have m_t). In this case, there will be 9 terms, each proportional to $-\frac{2R^2 \bar{Y}^2 v_4^2}{3}$, and it is important to realize that every one of them will be real and negative, because $(O_{u_R}^\dagger \frac{1}{\hat{F}_u^2} O_{u_R})_{33} \geq 0$. When $j = 2$ (m_c) there will be only 4 terms $\sim \frac{2R^2 \bar{Y}^2 v_4^2}{3}$ but every one of them will have generically a random complex phase (the 5 remaining terms are much smaller). For $j = 1$ (m_u) there is only one term $\sim \frac{2R^2 \bar{Y}^2 v_4^2}{3}$ contributing, with the other 8 terms being again suppressed. So at the end of the day the dominant contribution to a_{ii} will consist of 14 terms, 9 of which are

negative and the remaining 5 have random complex phases. Generically each of these terms are of the same size $\sim \frac{2R^2 \bar{Y}^2 v_4^2}{3}$ so from a statistical argument, $a_{ii} - 1$ should receive a negative contribution $\sim -9(\frac{2R^2 \bar{Y}^2 v_4^2}{3})$. This result is confirmed by the numerical scan presented below.

One can perform the same analysis for the element (22) of the Yukawa matrix and realize that in this case the number of terms aligned (contributing constructively) is 4, and for the (11) element there are none. This means that the largest corrections are expected in the third generation Yukawa couplings, with a suppressed correction in second generation couplings and much more suppressed correction for first generation couplings. This structure in the corrections seems to be a result of the hierarchical structure of the flavor anarchy setup.

Finally, we must remind the reader that it was crucial to take $Y_1 = Y_2$ (which is required in the Bulk Higgs scenario) to obtain these predictions. In the case $Y_1 \neq Y_2$, there will be no alignment of terms, and we therefore generally expect smaller corrections to the third generation Yukawa couplings.

B. Validity of $\bar{Y} v_4 R'$ expansion

We managed to solve the fermion equations by expanding them in the parameter $(\bar{Y}^2 v_4^2 R^2)$, and so our results can be trusted as long as

$$\bar{Y} \lesssim \frac{1}{v_4 R'} \quad (\sim 9 \text{ for } R'^{-1} = 1500 \text{ GeV}) \quad (84)$$

but we have seen in the previous subsection that the corrections to htt and hbb couplings do pick up an extra numerical factor of ~ 9 in the expansion parameter $(\bar{Y}^2 v_4^2 R^2)$. This means that, at least for third generation fermions, our approximation is valid only for

$$\bar{Y} \lesssim \frac{1}{v_4 R' \sqrt{9}} (\sim 3 \text{ for } R'^{-1} = 1500 \text{ GeV}). \quad (85)$$

Generically for the case with $\bar{Y} \gtrsim 3$ we will still have a large misalignment between the Higgs couplings and fermion masses but to be able to make valid predictions one would have to solve the equations of motion [Eq. (29) to (32)] exactly or use a different perturbative parameter. In the numerical analysis presented below we performed a scan with $0.3 < |Y_{1,2}^{5D}| < 3$, where our expansion is valid. We then also allowed for slightly larger values of the Yukawas such that $1 < |Y_{1,2}^{5D}| < 4$. The average size of the couplings is still below 3, so for a KK scale of $R'^{-1} = 1500$ GeV or above, the results will still be precise enough, although approaching the edge of perturbative convergence.

C. Numerical scan

We did a numerical scan over the input parameters $(Y_1^{5D})_{ij}$, $(Y_2^{5D})_{ij}$, c_{q_i} , c_{d_i} , c_{u_i} and we set $R'^{-1} = 1.5$ TeV.

In our scan, we pick the points that give the correct SM quark masses and Cabibbo-Kobayashi-Maskawa matrix. Then we calculate the 4D effective Yukawa couplings of Higgs with SM quarks. We present here only the results for $|Y_{1,2}^{5D}| \in [0.3, 3]$. First, we scan the set of parameters with $Y_1^{5D} = Y_2^{5D}$ which is motivated by bulk Higgs. Here are the results for this case:

$$a_{ij}^d = \begin{pmatrix} 0.99-1 & 0.006-0.019 & 0.004-0.012 \\ 0.006-0.019 & 0.96-0.99 & 0.007-0.02 \\ 0.042-0.10 & 0.075-0.18 & 0.85-0.93 \end{pmatrix} \quad (86)$$

$$a_{ij}^u = \begin{pmatrix} 0.99-1 & 0.06-0.16 & 0.09-0.21 \\ 0.003-0.008 & 0.94-0.98 & 0.03-0.09 \\ 0.009-0.02 & 0.05-0.14 & 0.71-0.82 \end{pmatrix}. \quad (87)$$

The first and second numbers are the 25% and 75% quantiles of the distribution of $|a_{ij}|$ obtained from the scan (i.e. 50% of all the values we obtained in the scan for each $|a_{ij}|$ lie between these two quantiles). From the results we can see that the values of $a_{ij}^{u,d}$ from the scan are consistent with the estimates presented above [Eq. (80) and (81)], and the expected reduction of $h\bar{t}t$ coupling is confirmed. We can also easily see this reduction of third generation Yukawa couplings in Fig. 3.

For the case when Y_1^{5D} and Y_2^{5D} are completely uncorrelated (Brane Higgs) we get the following results:

$$a_{ij}^d = \begin{pmatrix} 0.99-1 & 0.01-0.026 & 0.005-0.012 \\ 0.012-0.03 & 0.98-1.01 & 0.008-0.02 \\ 0.05-0.12 & 0.07-0.2 & 0.96-1.03 \end{pmatrix} \quad (88)$$

$$a_{ij}^u = \begin{pmatrix} 0.98-1.01 & 0.07-0.17 & 0.08-0.19 \\ 0.004-0.009 & 0.97-1.02 & 0.025-0.067 \\ 0.007-0.016 & 0.04-0.11 & 0.9-0.99 \end{pmatrix}. \quad (89)$$

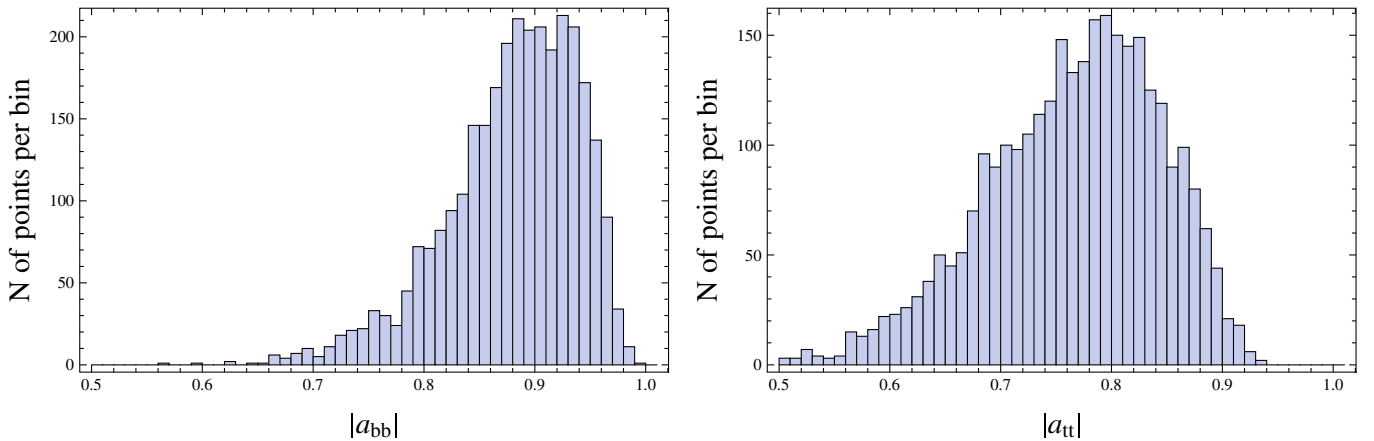


FIG. 3 (color online). Distribution of the absolute value of the normalized Higgs couplings to $t\bar{t}$ and $b\bar{b}$, a_{tt} and a_{bb} , in our numerical scan, with a fixed KK scale of $R'^{-1} = 1500$ GeV (KK gluon mass $M_{KKG} = 2.45R'^{-1}$) and for 5D Yukawa couplings $|Y_{5D}^{ij}| \in [0.3, 3]$. The expected generic suppression for both couplings is demonstrated numerically quite clearly.

We can see that the off-diagonal terms of $a_{ij}^{u,d}$ are of the same order as the previous case. However the diagonal entries do not have the suppression as in the $Y_1^{5D} = Y_2^{5D}$ case, see the discussion in Sec. VI A.

VII. LEPTON SECTOR

Generically one can see that the same effects will lead to Higgs flavor violation in the lepton sector; the only difference is that in the lepton sector there are various ways to explain the large mixing angles and light masses for the neutrinos [37–39]. Now we want to look at Higgs flavor violation in the charged lepton sector, then depending on a given neutrino model, the left-handed charged lepton profiles can be either hierarchical and UV localized (i), or similar and UV localized (ii). The profiles of the right-handed charged leptons are always hierarchical and localized near the UV brane. We treat these two cases separately.

- (i) Case (i)—left-handed and right-handed profiles are hierarchical. Then the profiles should satisfy the following relations:

$$f_L^i f_e^i \sim \frac{m_i^l}{\bar{Y} v_4}, \quad (90)$$

where $f_{L,e}$ are profiles of the left-handed and right-handed fields, respectively, then the generational mixing is also hierarchical

$$(O_{L,e})^{i,j} \sim \frac{f_{L,e}^i}{f_{L,e}^j}, \quad i < j. \quad (91)$$

We again parametrize our Lagrangian in the following form:

$$\mathcal{L}_{\text{HFV}} = a_{ij}^l \sqrt{\frac{m_i^l m_j^l}{v_4^2}} H \bar{L}^i e^j + \text{H.c.} \quad (92)$$

Where L, e are $SU(2)_L$ doublets and singlets, respectively, then we can estimate a_{ij}^l

$$a_{ij}^l \sim \frac{2}{3} \bar{Y}^2 (v_4^2 R'^2) \sqrt{\frac{f_L^i f_e^j}{f_L^j f_e^i}} \quad (93)$$

One can see that our estimate depends on the profiles of the fermions, but the following relation will be valid:

$$\begin{aligned} \sqrt{|a_{ij}^l|^2 + |a_{ji}^l|^2} &\geq \frac{4}{3} \bar{Y}^2 (v_4^2 R'^2) \\ &= 0.16 \left(\frac{1500 \text{ GeV}}{1/R'} \right)^2 \left(\frac{\bar{Y}}{3} \right)^2. \end{aligned} \quad (94)$$

This inequality is saturated when $\frac{f_L^i}{f_L^j} \sim \frac{f_e^i}{f_e^j} \sim \sqrt{\frac{m_i^l}{m_j^l}}$, i.e., when the hierarchy of charged lepton masses are explained equally by the profiles of left-handed and right-handed fields.

- (ii) Case (ii)—right-handed profiles are hierarchical and left-handed profiles are similar $f_L^1 \sim f_L^2 \sim f_L^3$. Then the profiles satisfy the following relations:

$$\begin{aligned} f_L^i f_e^i &\sim \frac{m_i^l}{\bar{Y} v_4} & \frac{f_L^i}{f_L^j} &\sim O(1), & i < j \\ \frac{f_e^i}{f_e^j} &\sim \frac{m_i^l}{m_j^l}, & i < j \end{aligned} \quad (95)$$

then we can estimate the parameter a_{ij}^l to be

$$\begin{aligned} a_{ij}^l &\sim \frac{2}{3} \bar{Y}^2 (v_4^2 R'^2) \sqrt{\frac{f_e^j}{f_e^i}} \\ &\sim 0.08 \left(\frac{1500 \text{ GeV}}{1/R'} \right)^2 \left(\frac{\bar{Y}}{3} \right)^2 \sqrt{\frac{m_j^l}{m_i^l}}. \end{aligned} \quad (96)$$

These flavor violating Higgs Yukawa couplings to leptons can also lead to interesting collider signals, which will also be discussed in the next section.

VIII. PHENOMENOLOGY

The FCNC generated by flavor violating Higgs Yukawa couplings will affect many low energy observables and also give possible signature at colliders. In this section, we first discuss bounds on Higgs flavor violation coming from $\Delta F = 2$ processes such as $\bar{K} - K$, $\bar{B} - B$, $\bar{D} - D$ mixing. And then we discuss possible signature at the LHC including suppression of htt coupling, rare top decay $t \rightarrow hc$ and flavor violating Higgs decay $h \rightarrow \tau\mu$.

A. Bounds from low energy physics

The $\Delta F = 2$ process can be described by the general Hamiltonian [40,41]

$$\mathcal{H}_{\text{eff}}^{\Delta F=2} = \sum_{a=1}^5 C_a Q_a^{q_i q_j} + \sum_{a=1}^3 \tilde{C}_a \tilde{Q}_a^{q_i q_j} \quad (97)$$

with

$$\begin{aligned} Q_1^{q_i q_j} &= \bar{q}_{jL}^\alpha \gamma_\mu q_{iL}^\alpha \bar{q}_{jL}^\beta \gamma^\mu q_{iL}^\beta, & Q_2^{q_i q_j} &= \bar{q}_{jR}^\alpha q_{iL}^\alpha \bar{q}_{jR}^\beta q_{iL}^\beta, \\ Q_3^{q_i q_j} &= \bar{q}_{jR}^\alpha q_{iL}^\beta \bar{q}_{jR}^\beta q_{iL}^\alpha, & Q_4^{q_i q_j} &= \bar{q}_{jR}^\alpha q_{iL}^\alpha \bar{q}_{jL}^\beta q_{iR}^\beta, \\ Q_5^{q_i q_j} &= \bar{q}_{jR}^\alpha q_{iL}^\beta \bar{q}_{jL}^\beta q_{iR}^\alpha, \end{aligned} \quad (98)$$

where α, β are color indices. The operators \tilde{Q}_a are obtained from Q_a by exchange $L \leftrightarrow R$. For $\bar{K} - K$, $\bar{B}_d - B_d$, $\bar{B}_s - B_s$, $\bar{D} - D$ mixing, $q_i q_j = sd, bd, bs$, and uc , respectively. Exchange of the Higgs can give rise to new contribution to C_2 , \tilde{C}_2 , and C_4 . This can be seen in Fig. 4, where Fig. 4(a) gives C_2 and \tilde{C}_2 ; Fig. 4(b) gives C_4 . These new contributions are

$$C_2^h = a_{ij}^2 \frac{m_i m_j}{v^2} \frac{1}{m_h^2} \quad (99)$$

$$\tilde{C}_2^h = a_{ji}^2 \frac{m_i m_j}{v^2} \frac{1}{m_h^2} \quad (100)$$

$$C_4^h = a_{ij} a_{ji} \frac{m_i m_j}{v^2} \frac{1}{m_h^2} \quad (101)$$

where m_h is the mass of physical Higgs. The model independent bound on the new physics contribution to these Wilson coefficients are given in [40]. We use the renormalization group equation from [42] and give the bounds renormalized at the scale $\mu_h = 200 \text{ GeV}$

$$\begin{aligned} \text{Im} C_K^2 &\leq \left(\frac{1}{7 \times 10^7 \text{ GeV}} \right)^2, \\ \text{Im} C_K^4 &\leq \left(\frac{1}{1.3 \times 10^8 \text{ GeV}} \right)^2, \end{aligned} \quad (102)$$

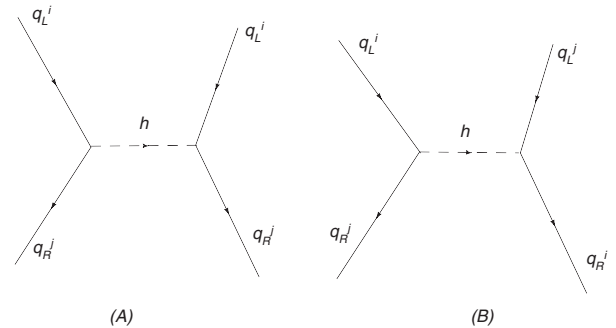


FIG. 4. Contribution to $\Delta F = 2$ processes from Higgs exchange.

$$\begin{aligned}
 |C_D^2| &\leq \left(\frac{1}{1.9 \times 10^6 \text{ GeV}} \right)^2, \\
 |C_D^4| &\leq \left(\frac{1}{2.9 \times 10^6 \text{ GeV}} \right)^2,
 \end{aligned} \tag{103}$$

$$\begin{aligned}
 |C_{B_d}^2| &\leq \left(\frac{1}{0.9 \times 10^6 \text{ GeV}} \right)^2, \\
 |C_{B_d}^4| &\leq \left(\frac{1}{1.4 \times 10^6 \text{ GeV}} \right)^2,
 \end{aligned} \tag{104}$$

$$\begin{aligned}
 |C_{B_s}^2| &\leq \left(\frac{1}{1 \times 10^5 \text{ GeV}} \right)^2, \\
 |C_{B_s}^4| &\leq \left(\frac{1}{1.7 \times 10^5 \text{ GeV}} \right)^2.
 \end{aligned} \tag{105}$$

These bounds put constraints on both the Higgs flavor violating Yukawa couplings parametrized by a_{ij} , and on the Higgs mass m_h . If we assume that the phases of $C_{2,4}^h$ are random, i.e., $\text{Im}(C_{2,4}^h) \sim |C_{2,4}^h|$, we can then rewrite the previous bounds as

$$\begin{aligned}
 0.25 \left(\frac{350 \text{ GeV}}{m_h} \right)^2 \frac{\text{Im}(a_{12}^d)^2}{(0.032)^2} &\leq 1, & 0.39 \left(\frac{350 \text{ GeV}}{m_h} \right)^2 \frac{\text{Im}(a_{21}^d)^2}{(0.04)^2} &\leq 1, & 1.11 \left(\frac{350 \text{ GeV}}{m_h} \right)^2 \frac{\text{Im}(a_{21}^d a_{12}^d)}{(0.032 \times 0.04)} &\leq 1 \\
 0.018 \left(\frac{350 \text{ GeV}}{m_h} \right)^2 \frac{|a_{12}^u|^2}{(0.15)^2} &\leq 1, & 0.00005 \left(\frac{350 \text{ GeV}}{m_h} \right)^2 \frac{|a_{21}^u|^2}{(0.008)^2} &\leq 1, & 0.0021 \left(\frac{350 \text{ GeV}}{m_h} \right)^2 \frac{|a_{12}^u a_{21}^u|}{(0.15 \times 0.008)} &\leq 1, \\
 0.0002 \left(\frac{350 \text{ GeV}}{m_h} \right)^2 \frac{|a_{13}^d|^2}{(0.01)^2} &\leq 1, & 0.03 \left(\frac{350 \text{ GeV}}{m_h} \right)^2 \frac{|a_{31}^d|^2}{(0.12)^2} &\leq 1, & 0.006 \left(\frac{350 \text{ GeV}}{m_h} \right)^2 \frac{|a_{13}^d a_{31}^d|}{(0.01 \times 0.12)} &\leq 1 \\
 0.00003 \left(\frac{350 \text{ GeV}}{m_h} \right)^2 \frac{|a_{23}^d|^2}{(0.01)^2} &\leq 1, & 0.003 \left(\frac{350 \text{ GeV}}{m_h} \right)^2 \frac{|a_{32}^d|^2}{(0.15)^2} &\leq 1, & 0.001 \left(\frac{350 \text{ GeV}}{m_h} \right)^2 \frac{|a_{32}^d a_{23}^d|}{(0.1 \times 0.01)} &\leq 1,
 \end{aligned}$$

where we compare the a_{ij} elements with their estimated values, for a fixed average Yukawa coupling $\bar{Y} = 2$ and KK scale given by $1/R' = 1500 \text{ GeV}$ [see formulas for the estimates from Eqs. (80) and (81)]. We also choose to compare the Higgs mass with a nominal value of $m_h = 350 \text{ GeV}$. We can see that the bound on $\text{Im}C_K^4$ coming from ϵ_K gives the strongest constraint on the Higgs mass. Specifically, we have

$$m_h \gtrsim 350 \text{ GeV} \quad \text{for } \text{Im}(a_{21}^d a_{12}^d) = (0.04 \times 0.032) \tag{106}$$

for a fixed KK scale of $1/R' = 1.5 \text{ TeV}$ and average 5D Yukawa of $\bar{Y}_{5D} = 2$.

In Fig. 5, we show the results of our numerical scan by plotting the bounds coming from ϵ_K in the $(m_h - M_{KKG})$ plane, where $M_{KKG} \approx 2.45R'^{-1}$ is the mass of the first KK gluon. In the left panel we show results for the case $|Y_{ij}^{5D}| \in [0.3, 3]$, and in the right panel we show results for the case $|Y_{ij}^{5D}| \in [1, 4]$. It can be seen quite clearly that a larger 5D Yukawa coupling leads to a higher bound on the KK scale. Note that the bounds coming from KK gluon exchange are inversely proportional to the size of the 5D Yukawa couplings \bar{Y}_{5D} . This leads to an interesting observation.

- (i) The new contribution to ϵ_K coming from Higgs exchange has opposite dependence on the 5D Yukawa coupling as that of KK gluon exchange. Thus, increasing the overall size of Y_{5D} will alleviate pressure from KK gluon exchange but, as we have

seen, this will also enhance the effect of Higgs mediated FCNCs.

With the chosen $\bar{Y}_{5D} (\sim 2)$, we can see that for the region of parameter space with $M_{KKG} \sim 3 \text{ TeV}$ (accessible at the LHC), a Higgs mass $m_h < 400 \text{ GeV}$ is disfavored. On the other hand, if a light ($< 150 \text{ GeV}$) Higgs is found in the LHC, we should expect sizable new physics contributions to $\Delta F = 2$ processes, just below current bounds.

B. Collider phenomenology

Besides low energy physics constraints, there could be very interesting signatures in colliders coming from the corrections to the Higgs Yukawa couplings. First of all, the reduction in the htt coupling, as argued in Sec. VI A and confirmed by our numerical scan, tells us that the Higgs production through gluon fusion will be generically suppressed (at least for the bulk Higgs scenario). This coupling can easily be suppressed by $\sim 25\%$ (for $R'^{-1} = 1.5 \text{ TeV}$ and $\bar{Y}_{5D} \sim 2$), and therefore the $gg \rightarrow h$ cross section will experience a reduction of 40% with respect to the expected SM value. This reduction in Higgs events from gluon fusion at the LHC can be observed quite clearly as well as the relative increase in importance of the production through gauge boson fusion [43]. We note again that the expected suppression is much larger in the case of a bulk Higgs, namely, when we have $Y_2 = Y_1$. In the case where Y_2 and Y_1 are unrelated, but with same overall size, there will not be a definitive prediction on the sign of the correction to the top Yukawa and bottom Yukawa couplings (i.e. there could be also enhancements), although

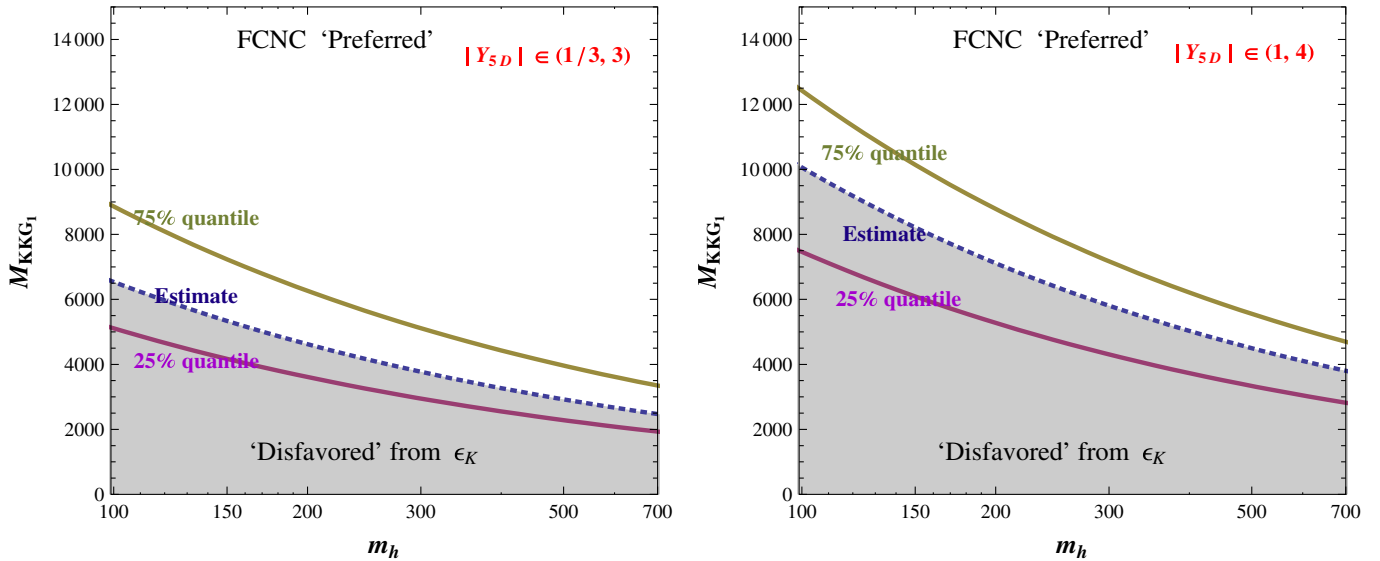


FIG. 5 (color online). Generic bounds in the plane (m_h, M_{KKG_1}) coming from ϵ_K due to tree-level Higgs exchange, where m_h is the Higgs boson mass and M_{KKG_1} is the mass of the first excited KK gluon. We perform a scan over 5D Yukawa matrices [such that $|Y_{5D}^{ij}| \in [0.3, 3]$ (left panel) and $|Y_{5D}^{ij}| \in [1, 4]$ (right panel)] and over fermion bulk c parameters. In the scan, we choose $Y_1^{5D} = Y_2^{5D}$ and take the $\beta \rightarrow \infty$ limit (the result has only a mild dependence on β). The 25% quantile and 75% quantile curves trace the points in this plane where 25% and 75% of the randomly generated parameter points are safe from Higgs mediated FCNCs (and are otherwise in agreement with the rest of experimental constraints in the scenario). The “estimate” curve is based on the expected size of Higgs flavor violating couplings [see Eqs. (80) and (81)] for the chosen range of the 5D Yukawas.

the size of the corrections is expected to be smaller than in the $Y_2 = Y_1$ case.

In the case of a light Higgs boson (and assuming that somehow low energy FCNC bounds are overcome), the branchings of the Higgs can change substantially due to the generically reduced hbb couplings. This would indirectly enhance the importance of $h \rightarrow \gamma\gamma$ signal, and maybe help overcome the overall reduction in the total production cross section due to reduced top Yukawa couplings. In Fig. 6, we plot the Higgs decay branching ratio for various final states versus the Higgs mass m_h .⁴ We can see clearly that for a light Higgs, the reduction in the hbb coupling changes the branching ratio to other channels significantly. For a heavy Higgs, the branching for $h \rightarrow tt$ is reduced.

If kinematically accessible ($m_h < m_t$), the flavor violating htc couplings will allow the decay $t \rightarrow ch$ to occur. The branching ratio of this process is given by (see for example [29])

$$\begin{aligned} \text{Br}(t \rightarrow ch) &= \frac{2(m_t^2 - m_h^2)^2 m_w^2}{(m_t^2 - m_w^2)^2 (m_t^2 + 2m_w^2) g_2^2} \\ &\times \left[|a_{23}^u|^2 + |a_{32}^u|^2 + \frac{4m_c m_t}{m_t^2 - m_h^2} \text{Re}[a_{23}^u a_{32}^u] \right] \\ &\times \frac{m_c m_t}{v^2}. \end{aligned} \quad (107)$$

If we take $m_h = 120$ GeV, then for $a_{23}^u \sim 0.08$ and $a_{32}^u \sim 0.14$, which are good estimates for $\bar{Y} = 2$ and a KK scale of

⁴We did not include $h \rightarrow \mu\tau$ mode on the plot because it is model dependent.

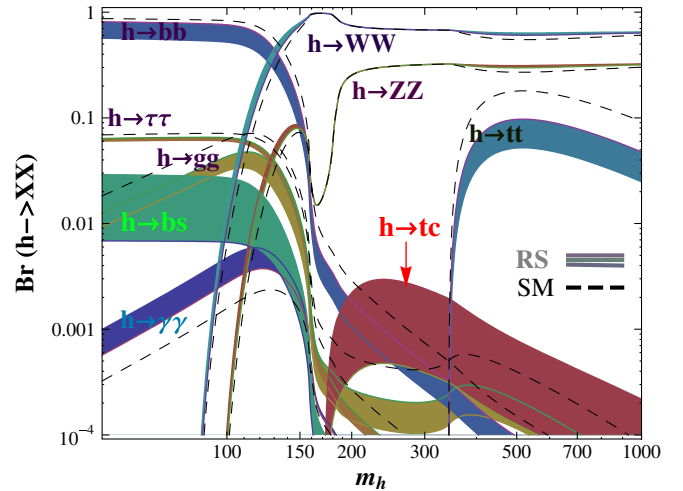


FIG. 6 (color online). Higgs decay branching fractions as a function of its mass, for the case of 5D Yukawas such that $|Y_{5D}^{ij}| \in [1, 4]$ and for a KK scale $R'^{-1} = 1500$ GeV ($M_{KKG_1} = 2.45R'^{-1}$). The dashed curves represent the SM branching fractions, and the color bands correspond to 25% and 75% quantiles of our scan results. The $h \rightarrow tt$ curve shows a suppressed branching due to suppressed htt couplings. This same type of suppression happens in the hbb couplings, which in turn enhances important channels such as $h \rightarrow \gamma\gamma$. Of course Higgs production through gluon fusion is also suppressed due to suppressed htt couplings, but vector boson fusion is assumed to remain as in the SM, allowing one to probe at the LHC these relative changes in the couplings. We note also the appearance of two new important channels, $h \rightarrow bs$ and $h \rightarrow tc$, the second of which could be looked at the LHC if the Higgs happens to be discovered (in the ZZ channel) in the appropriate mass regime.

$1/R' = 1500$ GeV [see Eq. (81)], we obtain a branching ratio of

$$\text{Br}(t \rightarrow ch) \sim 5 \times 10^{-5}. \quad (108)$$

The sensitivity of LHC for this rare top decay is $\text{Br}(t \rightarrow ch) \geq 6.5 \times 10^{-5}$ [44], precisely in the ballpark of our estimate. In Fig. 7 we show the results of our two scans, each with a different average size of the 5D Yukawas. It is shown that observing the signal at the LHC is quite possible although it requires larger Yukawa couplings and a light Higgs. If observed, this signal would be very valuable in determining the structure of the 5D setup.

Another interesting collider signature for light Higgs might be the Higgs lepton flavor violating decay $h \rightarrow \mu\tau$ [45,46]. The LHC reach for this process was studied in [45] and it could be observable if $|a_{\mu\tau}, (a_{\tau\mu})| > 0.15$. One can see from Eqs. (94) and (96) that for case (i), this decay is observable only for fairly large \bar{Y} (≥ 3) and low KK scale $1/R' \leq 1.5$ TeV, while for case (ii) there is an extra enhancement factor of $\sqrt{\frac{m_\tau}{m_\mu}} \sim 4$ for $a_{\mu\tau}$, so that in this case we expect larger parameter space to give us observable effects in the $h \rightarrow \mu\tau$ decay.

For a heavy Higgs ($m_h > m_t$), an interesting signal at the LHC might be the Higgs flavor violating decay $h \rightarrow tc$. A similar study on tc production from radion decay was considered in [47]. From Fig. 6 we can see that the branching for $h \rightarrow tc$ is in the range of 10^{-3} for a Higgs mass between 200–300 GeV, and for the favorable parameter values of $\bar{Y}_{5D} \sim 2$ and $1/R' = 1500$ GeV. However, even with a branching fraction of 10^{-3} the signal would most likely be dominated by large backgrounds at the LHC. Larger flavor violating couplings are still possible for even larger values of the 5D Yukawas, although calculability and perturbativity become then a greater issue. More

detailed analysis of the possibility and feasibility of this channel is left for future studies.

We finally must mention that in these models one generically expects the appearance of another light scalar in the spectrum—the radion graviscalar. As was pointed out in [47] the radion will also typically couple to fermions with off-diagonal couplings, and moreover, the two scalars could actually mix [48] giving rise to interesting changes in both Higgs and radion phenomenology [48–51]. In that situation, the physical states emerging from the mixing will inherit an admixture of the couplings of the original Higgs and radion, including their off-diagonal couplings to fermions. It would be interesting to revisit the phenomenology of Higgs-radion mixing in view of the results obtained in this paper, although we will leave this study for future investigations.

IX. CONCLUSION

In this article, we computed the misalignment between Higgs Yukawa couplings and SM fermion masses in the framework of warped extra dimensions. We estimated this misalignment in the mass insertion approximation and then calculated it by solving the fermion wave functions in 5D. An important result is that the main contributions to this misalignment are of the same order in both bulk and brane Higgs scenarios, which means that our results are general and independent of the Higgs localization. We first showed this fact in the bulk Higgs case by taking the Higgs to be infinitely localized towards the IR brane ($\beta \rightarrow \infty$); and then we also treated the brane Higgs case, with a suitably regularized delta function localization. A subtlety in doing the mass insertion approximation in the brane Higgs case is also discussed.

This misalignment generally leads to FCNC mediated by the Higgs boson. We estimated the size of these flavor changing Yukawa couplings in models with flavor anarchy. And we confirmed our estimates by scanning over the parameter space which reproduces the correct quark masses and mixing angles. In addition, we found that the Yukawa couplings of the third generation are generically suppressed relative to their SM values.

These flavor changing Yukawa couplings have important phenomenology implications. First, they lead to new contributions to flavor changing low energy observables and thus give us bounds on parameters of the Higgs sector. We found that ϵ_K gives the strongest bound which disfavors a light physical Higgs. In addition, these flavor changing Yukawa couplings can give us interesting signals at colliders. We discussed the possible reduction of Higgs production cross section and the changes in Higgs decay branchings at the LHC (including interesting new decay channels such as $h \rightarrow \mu\tau$ and $h \rightarrow tc$). Another interesting signal is the rare top decay $t \rightarrow ch$. We found that in a sizable part of the parameter space this decay can be seen at the LHC.

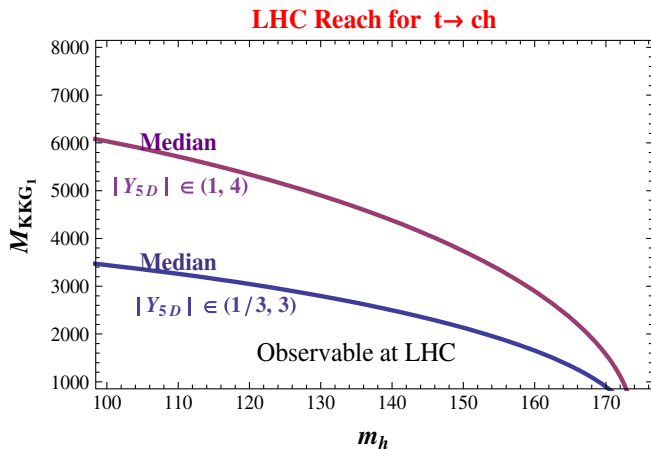


FIG. 7 (color online). LHC observability of the exotic decay of the top quark $t \rightarrow ch$ in the plane (m_h, M_{KKG_1}) . The two curves trace the region such that 50% of the generated points in our two scans (one with $|Y_{5D}^{ij}| \in [0.3, 3]$ and another with $|Y_{5D}^{ij}| \in [1, 4]$) will have a visible signal at the LHC.

ACKNOWLEDGMENTS

We would like to thank Raman Sundrum for interesting discussions, and specially Kaustubh Agashe for his encouragement, comments, and suggestions. A. A. was partially funded by NSF No. PHY-0652363.

APPENDIX A: GENERAL MISALIGNMENT FORMULAS

Here we present the result for the misalignment for general fermions (both UV and IR localized). The largest contribution [second term of Eq. (40)] is

$$\begin{aligned} \Delta_1^d = 2m_d^3 R^2 \frac{2 + c_d - c_q + \beta}{(1 + 2c_d)(1 - 2c_q)} & \left[\frac{\epsilon^{1+2c_d}}{3 - c_d - c_q + \beta} - \frac{1}{4 + c_d - c_q + \beta} - \frac{\epsilon^{2-2c_q+2c_d}}{3 - c_d - c_q + \beta} + \frac{\epsilon^{-2c_q+1}}{3 + c_d + c_q + \beta} \right. \\ & - \frac{\epsilon^{-2c_q+2c_d+2}}{4 + 2\beta} (\epsilon^{-1-2c_d} - 1) - \frac{\epsilon^{-2c_q+2c_d+2}}{4 + 2\beta} (\epsilon^{-1+2c_q} - 1) + \frac{\epsilon^{2c_d+1}}{5 - 2c_q + 2\beta} (\epsilon^{-1-2c_d} - 1) \\ & \left. + \frac{\epsilon^{-2c_q+1}}{5 + 2c_d + 2\beta} (\epsilon^{-1+2c_q} - 1) + \frac{\epsilon^{2+2c_d-2c_q}}{6 + c_d - c_q + 3\beta} (\epsilon^{-1-2c_d} - 1)(\epsilon^{-1+2c_q} - 1) \right]. \end{aligned} \quad (\text{A1})$$

For the case of the UV localized fermions ($c_q > 0.5$, $c_d < -0.5$) the 3rd, 4th, and 9th terms are dominating and we recover Eq. (47). For the subleading contribution of the misalignment Δ_2^d [first term of Eq. (40)] we get:

$$\begin{aligned} \Delta_2^d = \frac{m_d^3 R^2}{1 - 2c_q} & \left[-\frac{1 - \epsilon^2}{\epsilon^{2c_q-1} - 1} + \frac{\epsilon^{2c_q-1} - \epsilon^2}{(\epsilon^{2c_q-1} - 1)(3 - 2c_q)} + \frac{\epsilon^{1-2c_q} - \epsilon^2}{(1 + 2c_q)(\epsilon^{2c_q-1} - 1)} - \frac{1}{4 + c_d - c_q + \beta} \right. \\ & \left. + \frac{2\epsilon^{1-2c_q}}{3 + c_q + c_d + \beta} + \frac{(\epsilon^{2c_q-1} - 1)\epsilon^{1-2c_q}}{5 + 2c_d + 2\beta} + (c_{d,q} \leftrightarrow -c_{q,d}) \right]. \end{aligned} \quad (\text{A2})$$

For the UV localized fermions ($c_q > 0.5$, $c_d < -0.5$) the 3rd, 5th, and 6th terms are important and we recover Eq. (48).

APPENDIX B: MISALIGNMENT DUE TO

$$v(z) \neq h(z)$$

In this section we discuss the possible flavor violation coming from the misalignment between the physical Higgs profile and the Higgs vev profile. The profile of the KK Higgs modes are given by [32]

$$h_m(z) = Bz^2(Y_{1+\beta}(mR)J_\beta(mz) + J_{1+\beta}(mR)Y_\beta(mz)), \quad (\text{B1})$$

where the mass of the KK mode is determined by the boundary conditions. Then for the lightest mode (physical Higgs) we can expand the Bessel functions using ($m \ll 1/z$)

$$h(z) = A(m_H)z^{2+\beta} \left(1 - \frac{m_H^2 z^2}{4(\beta + 1)} \right) \quad (\text{B2})$$

where the constant $A(m_H)$ is fixed by requiring the Higgs profile normalization. One can see that in the limit ($m_H = 0$), the profiles of the physical Higgs and the profile of its vev become proportional to each other. Then, the normalization constants of the Higgs field and the Higgs vev, $A(m_H)$ and $V(\beta)$ [Eq. (22)], will be related by

$$A(m_H)|_{m_H=0} \equiv A(0) = \frac{V(\beta)}{v_4} \quad (\text{B3})$$

and so the profile of the Higgs will be given by

$$\begin{aligned} h(z) &= A(0)z^{2+\beta} \left[1 + \frac{m_H^2 R^2}{2(4 + \beta)} - \frac{m_H^2 z^2}{4(1 + \beta)} \right. \\ & \left. + O((m_H^2 R^2)^2) \right] \\ &= \frac{v(z)}{v_4} \left[1 + \frac{m_H^2 R^2}{2(4 + \beta)} - \frac{m_H^2 z^2}{4(1 + \beta)} + O((m_H^2 R^2)^2) \right]. \end{aligned} \quad (\text{B4})$$

This will lead to a new contribution to the shift Δ^d

$$\begin{aligned} \Delta_3^d &= -m_d(m_H^2 R^2) \left[\frac{1}{2(4 + \beta)} \right. \\ & \left. - \frac{2 + \beta + c_d - c_q}{4(1 + \beta)(4 + \beta + c_d - c_q)} \right], \end{aligned} \quad (\text{B5})$$

but one can see that in the limit $\beta \rightarrow \infty$ this contribution decouples. Moreover, even for finite β , the numerical size of this type of flavor misalignment is small.

APPENDIX C: CONVERGENT INFINITE SUM IN THE MASS INSERTION APPROXIMATION

In this appendix, we address again the ‘‘contradiction’’ between the mass insertion approximation and the 5D calculation when the Higgs is on the IR brane. We will prove that one can obtain the result of Eq. (67) from direct calculations of the Feynman diagrams in the insertion approximation.

Naively, the importance of the Y_2 term looks counter-intuitive because the profiles q_R , d_L do vanish at IR brane. Indeed if one follows the insertion approximation (see

Fig. 1) then the coupling between q_R^{KK} , d_L^{KK} and the Higgs vanish, so there will be no contribution to fermion masses and Yukawa couplings out of that diagram. However there is a subtlety in this approach, since we are expanding in KK modes by using the profiles for the case $\langle H \rangle = 0$. This means that after electroweak symmetry breaking, we should include the mixing between the whole tower of KK modes induced by a nonzero Higgs vev. Naively the heavier KK modes should decouple so that their contribution should not qualitatively affect the final result. But this appears not to be the case.

For simplicity we will start our discussion from the case of a flat extra dimension. Now, the fermion profiles are given by sine and cosine functions instead of Bessel functions, and the derivation becomes much more transparent. At the same time when the Higgs is localized on one of the branes, we still have the same issue for any Yukawa coupling between odd modes and the Higgs i.e., the term $Y_2 q_R d_L$ naively should not lead to any misalignment between fermion masses and Yukawa couplings.

The profiles of the even KK modes are given by

$$q_L^n(d_R^n) = \frac{1}{\sqrt{\pi R}} \cos\left(\frac{nz}{R}\right), \quad n = \pm 1, \pm 2, \dots \quad (C1)$$

$$q_L^0(d_R^0) = \frac{1}{\sqrt{2\pi R}}$$

and the odd KK mode profiles are

$$q_R^n = \frac{1}{\sqrt{\pi R}} \sin\left(\frac{nz}{R}\right) \quad n = \pm 1, \pm 2, \dots \quad (C2)$$

$$d_L^n = -\frac{1}{\sqrt{\pi R}} \sin\left(\frac{nz}{R}\right) \quad n = \pm 1, \pm 2, \dots$$

The coupling $Y_2 H Q_R D_L \delta(y - \pi R)$ should vanish because Q_R and D_L are vanishing at $y = \pi R$, but in the diagram (Fig. 1) we have to include all the KK modes, so we will have an infinite sum of zeroes, and in order to treat all the infinities accurately we will again use the rectangular regulator Eq. (58) for the delta function.

Let us define the following quantities:

$$Y_{mn}^e - \text{coupling between "m" and "n" even KK modes}$$

$$Y_{mn}^o - \text{coupling between "m" and "n" odd KK modes} \quad (C3)$$

then

$$Y_{mn}^e = \frac{(-1)^{m+n}}{2\pi\epsilon} \left[\frac{\sin\left(\frac{(n-m)\epsilon}{R}\right)}{n-m} + \frac{\sin\left(\frac{(n+m)\epsilon}{R}\right)}{n+m} \right]$$

$$= \frac{(-1)^{n+m}}{2\pi R} \left[1 + O\left((n, m)^2 \left(\frac{\epsilon}{R}\right)^2\right) \right],$$

$$Y_{mn}^o = -\frac{(-1)^{m+n}}{2\pi\epsilon} \left[\frac{\sin\left(\frac{(n-m)\epsilon}{R}\right)}{n-m} - \frac{\sin\left(\frac{(n+m)\epsilon}{R}\right)}{n+m} \right]$$

$$= -\frac{(-1)^{n+m}}{3\pi R} \left(\frac{\epsilon}{R}\right)^2 mn \left[1 + O\left((n, m)^4 \left(\frac{\epsilon}{R}\right)^4\right) \right]. \quad (C4)$$

In a similar way one can calculate the coupling between the 0 and the n th even KK modes

$$Y_{0n}^e = Y_1 \frac{(-1)^n \sin\left(\frac{n\epsilon}{R}\right)}{\pi\sqrt{2}\epsilon} = Y_1 \frac{(-1)^n}{\pi\sqrt{2}R} \left[1 + O\left(\frac{n\epsilon}{R}\right) \right]. \quad (C5)$$

As we said before to find the $O(v^3 R^2)$ misalignment between fermion masses and Yukawa couplings, it is sufficient to consider the contribution of the diagram with three Higgs insertions (see Fig. 1) and sum over all KK modes. However, for KK modes with $|n|, |m| \geq R/\epsilon$, the sinusoidal oscillation of the odd wave function inside the Higgs profile will tend to make the $Y_{m,n}^o$ coupling vanish. Thus we need to sum up $|n|, |m|$ only up to $\sim R/\epsilon$, and the estimate of that sum will be

$$\Delta_1^d \sim v^2 \sum_{|n|, |m|=1}^{R/\epsilon} Y_{0n}^e \frac{R}{n} Y_{nm}^o \frac{R}{m} Y_{0m}^e \sim \frac{Y_1^2 Y_2 v^2}{R} \sum_{n, m=1}^{R/\epsilon} \left(\frac{\epsilon}{R}\right)^2. \quad (C6)$$

One can see that all of the terms up to $n \leq R/\epsilon$ are of the same order, and so the sum should be finite and proportional to $\frac{Y_1^2 Y_2 v^2}{R}$. Exact resummation gives us

$$\Delta_1^d = \frac{Y_1^2 Y_2 v^3}{6\pi R}. \quad (C7)$$

It is important to mention that to account for the flavor mixing effects one has to sum at least the first R/ϵ terms. And the lightest mode is an admixture of the zero mode and the first R/ϵ KK modes. This should not be surprising because the zero Higgs vev expansion should include all KK modes up to the value of the cutoff and the cutoff is related to the inverse of the Higgs wave function width. In our case the width of the Higgs profile is ϵ so we have to sum all the modes with masses up to $1/\epsilon$.

In the case of the warped geometry things become a little bit more complicated, because the sine and cosine are replaced by the Bessel functions

$$f^e(z, m_n) = (Rz)^{5/2} \frac{1}{N\sqrt{R \ln(R'/R)}} [J_\alpha(m_n z) + b_\alpha(m_n) Y_\alpha(m_n z)] \quad (C8)$$

$$f^e(z, m_n) = (Rz)^{5/2} \frac{1}{N\sqrt{R \ln(R'/R)}} [J_{\alpha-1}(m_n z) + b_\alpha(m_n) Y_{\alpha-1}(m_n z)]$$

where

$$\alpha = c + \frac{1}{2} \quad b_\alpha(m_n) = \frac{J_{\alpha-1}(m_n R)}{Y_{\alpha-1}(m_n R)} = \frac{J_{\alpha-1}(m_n R')}{Y_{\alpha-1}(m_n R')} \quad (C9)$$

but for the cases when the mass of the KK mode is $\frac{1}{R'} \ll m \ll \frac{1}{R}$ the expressions for the profiles simplify signifi-

cantly

$$\begin{aligned}
m_n R' &\sim \pi(n + c/2 + 1/2) \\
J_\alpha(m_n z) &\sim \sqrt{\frac{2}{\pi m_n z}} \cos(m_n z - \pi/2(c + 1)) \\
J_{\alpha-1}(m_n z) &\sim \sqrt{\frac{2}{\pi m_n z}} \cos(m_n z - \pi/2c)
\end{aligned} \tag{C10}$$

so the ratio

$$\left. \frac{f^o(z, m_n)}{f^e(z, m_n)} \right|_{z=R'-\varepsilon} \sim \frac{\sin(m_n \varepsilon)}{\cos(m_n \varepsilon)} \sim \sin(m_n \varepsilon) \tag{C11}$$

and so it becomes obvious that

$$Y_{nl}^o \sim \sin(m_n \varepsilon) \sin(m_l \varepsilon). \tag{C12}$$

One can see that Y_{nl}^o has the same dependence on the KK numbers as in the flat case, and on the masses of the KK modes $m_n \sim \pi n/R'$ for large n , so the calculation for the warp geometry will proceed exactly as in the flat geometry case.

There is yet another way to understand this result.⁵ Instead of operator $Y_2 H \bar{u}_L q_R$ we can consider the following effective operator localized at the IR brane:

⁵We thank Raman Sundrum for suggesting it.

$$\frac{Y_2(\partial_z \bar{u}_L)(\partial_z q_R) H \delta(z - R')}{\Lambda^2}. \tag{C13}$$

Then the contribution to the diagram (Fig. 1) will be

$$\begin{aligned}
\Delta_1^d &\sim \sum_{n,l \leq (\Lambda/M_{\text{kk}})} \frac{Y_1 v}{m_n} \frac{Y_2 m_n m_l}{\Lambda^2} \frac{Y_1 v}{m_l} \\
&\sim \frac{Y_1^2 Y_2 v^2}{\Lambda^2} \sum_{n,l \leq (\Lambda/M_{\text{kk}})} \sim \frac{Y_1^2 Y_2 v^2}{M_{\text{kk}}^2}
\end{aligned} \tag{C14}$$

and we can see that the effect of every KK mode becomes equally important and we again have to sum up all the modes up to the value of the cutoff Λ , obtaining a cutoff independent finite result. On the other hand it is easily seen that this operator corresponds to giving Higgs some finite width $\sim \frac{1}{\Lambda}$. Indeed if will use the boundary conditions for the profiles $u_L|_{R'} = q_R|_{R'} = 0$ we will get

$$-\left. \frac{\partial_z \bar{u}_L}{\Lambda} \right|_{R'} = \left(\bar{u}_L - \frac{\partial_z \bar{u}_L}{\Lambda} \right)_{R'} = \bar{u}_L \left(R' - \frac{1}{\Lambda} \right) + O\left(\frac{1}{\Lambda^2} \right) \tag{C15}$$

so the operator (C13) is equivalent to

$$\frac{(\partial_z \bar{u}_L)(\partial_z q_R) H \delta(z - R')}{\Lambda^2} \Leftrightarrow (\bar{u}_L q_R) H \delta\left(z - R' - \frac{1}{\Lambda} \right). \tag{C16}$$

This result is not surprising because the width of the Higgs profile should be related to the value of the inverse cutoff.

-
- [1] L. Randall and R. Sundrum, Phys. Rev. Lett. **83**, 3370 (1999); arXiv:hep-ph/9905221; Phys. Rev. Lett. **83**, 4690 (1999).
- [2] T. Gherghetta and A. Pomarol, Nucl. Phys. **B586**, 141 (2000); arXiv:hep-ph/0003129; Y. Grossman and M. Neubert, Phys. Lett. B **474**, 361 (2000); arXiv:hep-ph/9912408.
- [3] H. Davoudiasl, J. L. Hewett, and T. G. Rizzo, Phys. Lett. B **473**, 43 (2000); A. Pomarol, Phys. Lett. B **486**, 153 (2000); S. Chang, J. Hisano, H. Nakano, N. Okada, and M. Yamaguchi, Phys. Rev. D **62**, 084025 (2000).
- [4] K. Agashe, A. Delgado, M. J. May, and R. Sundrum, J. High Energy Phys. 08 (2003) 050.
- [5] K. Agashe, R. Contino, and A. Pomarol, Nucl. Phys. **B719**, 165 (2005).
- [6] K. Agashe and R. Contino, Nucl. Phys. **B742**, 59 (2006); M. Carena, E. Ponton, J. Santiago, and C. E. M. Wagner, Nucl. Phys. **B759**, 202 (2006); Phys. Rev. D **76**, 035006 (2007); R. Contino, L. Da Rold, and A. Pomarol, Phys. Rev. D **75**, 055014 (2007); A. D. Medina, N. R. Shah, and C. E. M. Wagner, Phys. Rev. D **76**, 095010 (2007); C. Bouchart and G. Moreau, Nucl. Phys. **B810**, 66 (2009).
- [7] K. Agashe, R. Contino, L. Da Rold, and A. Pomarol, Phys. Lett. B **641**, 62 (2006).
- [8] K. Agashe, G. Perez, and A. Soni, Phys. Rev. D **71**, 016002 (2005); K. Agashe, M. Papucci, G. Perez, and D. Pirjol, arXiv:hep-ph/0509117.
- [9] S. J. Huber and Q. Shafi, Phys. Lett. B **498**, 256 (2001).
- [10] C. Csaki, A. Falkowski, and A. Weiler, J. High Energy Phys. 09 (2008) 008; arXiv:0804.1954.
- [11] M. Blanke, A. J. Buras, B. Duling, S. Gori, and A. Weiler, J. High Energy Phys. 03 (2009) 001.
- [12] A. L. Fitzpatrick, G. Perez, and L. Randall, arXiv:0710.1869.
- [13] S. Davidson, G. Isidori, and S. Uhlig, Phys. Lett. B **663**, 73 (2008).
- [14] M. E. Albrecht, M. Blanke, A. J. Buras, B. Duling, and K. Gemmler, arXiv:0903.2415.
- [15] K. Agashe, A. Belyaev, T. Krupovnickas, G. Perez, and J. Virzi, Phys. Rev. D **77**, 015003 (2008); B. Lillie, L. Randall, and L. T. Wang, J. High Energy Phys. 09 (2007) 074; B. Lillie, J. Shu, and T. M. P. Tait, Phys. Rev. D **76**, 115016 (2007); A. Djouadi, G. Moreau, and R. K. Singh, Nucl. Phys. **B797**, 1 (2008); M. Guchait, F. Mahmoudi, and K. Sridhar, Phys. Lett. B **666**, 347 (2008); U. Baur and L. H. Orr, Phys. Rev. D **76**, 094012 (2007);

- 77, 114001 (2008); M. Carena, A. D. Medina, B. Panes, N. R. Shah, and C. E. M. Wagner, *Phys. Rev. D* **77**, 076003 (2008).
- [16] K. Agashe *et al.*, *Phys. Rev. D* **76**, 115015 (2007); K. Agashe, S. Gopalakrishna, T. Han, G-Y. Huang, and A. Soni, arXiv:0810.1497.
- [17] G. Moreau and J. I. Silva-Marcos, *J. High Energy Phys.* 03 (2006) 090.
- [18] G. Cacciapaglia, C. Csaki, J. Galloway, G. Marandella, J. Terning, and A. Weiler, *J. High Energy Phys.* 04 (2008) 006; M. C. Chen and H. B. Yu, *Phys. Lett. B* **672**, 253 (2009); G. Perez and L. Randall, arXiv:0805.4652; C. Csaki, C. Delaunay, C. Grojean, and Y. Grossman, *J. High Energy Phys.* 10 (2008) 055; J. Santiago, *J. High Energy Phys.* 12 (2008) 046; C. Csaki, Y. Grossman, G. Perez, Z. Surujon, and A. Weiler (unpublished).
- [19] C. Csaki, A. Falkowski, and A. Weiler, *Phys. Rev. D* **80**, 016001 (2009).
- [20] K. Agashe, A. Azatov, and L. Zhu, *Phys. Rev. D* **79**, 056006 (2009).
- [21] O. Gedalia, G. Isidori, and G. Perez, arXiv:0905.3264.
- [22] K. Agashe, A. E. Blechman, and F. Petriello, *Phys. Rev. D* **74**, 053011 (2006).
- [23] K. Agashe and R. Contino, arXiv:0906.1542.
- [24] W. Buchmuller and D. Wyler, *Nucl. Phys.* **B268**, 621 (1986).
- [25] F. del Aguila, M. Perez-Victoria, and J. Santiago, *Phys. Lett. B* **492**, 98 (2000); *J. High Energy Phys.* 09 (2000) 011.
- [26] K. S. Babu and S. Nandi, *Phys. Rev. D* **62**, 033002 (2000).
- [27] G. F. Giudice and O. Lebedev, *Phys. Lett. B* **665**, 79 (2008).
- [28] K. Agashe, G. Perez, and A. Soni, *Phys. Rev. D* **75**, 015002 (2007).
- [29] S. Casagrande, F. Goertz, U. Haisch, M. Neubert, and T. Pfoh, *J. High Energy Phys.* 10 (2008) 094.
- [30] A. J. Buras, B. Duling, and S. Gori, arXiv:0905.2318.
- [31] C. Csaki, C. Grojean, J. Hubisz, Y. Shirman, and J. Terning, *Phys. Rev. D* **70**, 015012 (2004).
- [32] G. Cacciapaglia, C. Csaki, G. Marandella, and J. Terning, *J. High Energy Phys.* 02 (2007) 036.
- [33] H. Davoudiasl, B. Lillie, and T. G. Rizzo, *J. High Energy Phys.* 08 (2006) 042.
- [34] B. Batell, T. Gherghetta, and D. Sword, *Phys. Rev. D* **78**, 116011 (2008).
- [35] A. Delgado and D. Diego, *Phys. Rev. D* **80**, 024030 (2009).
- [36] S. M. Aybat and J. Santiago, arXiv:0905.3032.
- [37] G. Perez and L. Randall, *J. High Energy Phys.* 01 (2009) 077.
- [38] K. Agashe, T. Okui, and R. Sundrum, *Phys. Rev. Lett.* **102**, 101801 (2009).
- [39] K. Agashe, arXiv:0902.2400.
- [40] M. Bona *et al.* (UTfit Collaboration), *J. High Energy Phys.* 03 (2008) 049.
- [41] A. J. Buras, arXiv:hep-ph/9806471.
- [42] J. A. Bagger, K. T. Matchev, and R. J. Zhang, *Phys. Lett. B* **412**, 77 (1997).
- [43] G. L. Bayatian *et al.* (CMS Collaboration), *J. Phys. G* **34**, 995 (2007); ATLAS Collaboration, CERN Report No. CERN-OPEN-2008-020, Geneva, 2008 (unpublished).
- [44] J. A. Aguilar-Saavedra and G. C. Branco, *Phys. Lett. B* **495**, 347 (2000).
- [45] T. Han and D. Marfatia, *Phys. Rev. Lett.* **86**, 1442 (2001).
- [46] J. L. Diaz-Cruz and J. J. Toscano, *Phys. Rev. D* **62**, 116005 (2000).
- [47] A. Azatov, M. Toharia, and L. Zhu, *Phys. Rev. D* **80**, 031701 (2009).
- [48] G. F. Giudice, R. Rattazzi, and J. D. Wells, *Nucl. Phys.* **B595**, 250 (2001).
- [49] C. Csáki, M. L. Graesser, and G. D. Kribs, *Phys. Rev. D* **63**, 065002 (2001).
- [50] S. Bae, P. Ko, H. S. Lee, and J. Lee, *Phys. Lett. B* **487**, 299 (2000); K. Cheung, *Phys. Rev. D* **63**, 056007 (2001); J. L. Hewett and T. G. Rizzo, *J. High Energy Phys.* 08 (2003) 028; D. Dominici, B. Grzadkowski, J. F. Gunion, and M. Toharia, *Nucl. Phys.* **B671**, 243 (2003); *Acta Phys. Pol. A* **33**, 2507 (2002); J. F. Gunion, M. Toharia, and J. D. Wells, *Phys. Lett. B* **585**, 295 (2004).
- [51] M. Toharia, *Phys. Rev. D* **79**, 015009 (2009).